POLITECNICO DI MILANO

Scuola di Ingegneria Industriale e dell'Informazione

Corso di Laurea Magistrale in
Ingegneria Energetica

Hydrogen storage for variable renewable electricity integration:
Techno-economic analysis of a Lined Rock Cavern system

Relatore: Prof. Stefano Campanari

Correlatore: Prof. Filip Johnsson, Chalmers University of Technology

Tesi di Laurea di:

Giuseppe RIPEPI Matr. 852597

Anno Accademico 2016 - 2017

Abstract

The following study has been developed in cooperation with Chalmers University of Technology, during an internship in the Energy Division of the Hearth, Space and Environment Department of the same university. The work has been reviewed and discussed within the division and has been mainly followed by the Sustainable European Energy Systems group members Filip Johnsson (co-rapporteur) and Viktor Johansson (PhD student). Finally the thesis was informally defended within the Energy Division.

INTRODUCTION

In a future with increasing focus on emissions reduction and industry decarbonization, large-scale energy storage systems will be at the top of the research and development process. There will be the need to smooth electricity production profiles due to an increased renewable energy sources (RES) penetration, which will not probably be managed with the already existing flexibility measures. While some of the storage technologies are already well known and in operation, most of them are only at their early stage of development or even at the research stage. Among the technologies under development it is possible to locate hydrogen storage in all its forms; in particular underground hydrogen storage is seen as a promising technology that can exploit already known gas storage technology. With a particular attention to lined underground rock cavern (LRC) for hydrogen storage, this study aims to understand the hydrogen storage potential in the development of the future energy systems, through a techno-economic analysis of a system of LRC. While this technology poses a challenge in terms of lining an underground cavern and operate it (the only similar application in operation is a natural gas storage plant based on a LRC system in Skallen, Sweden), on the other hand the excavation process and hydrogen handling are well known procedures, as well as there are several operative hydrogen storage salt caverns worldwide, which can provide specific expertise for the cavern operation. The construction of a LRC system for hydrogen storage would be a challenge in terms of putting together diverse expertise but, as shown by the Skallen facility and the ANGAS project developed by the Japan Gas Association (JPA), this is already possible.

The actual definition of large-scale energy storage systems is based on the maximum, already deployed systems capacities: they can reach the range of $1-2$GWh, coupled with a power rating of up to 200MW(see figure 1.1) and the only available technologies able to provide those characteristics are compressed air energy storage

(CAES) and pumped hydroelectric storage (PHS). However gas storage (as natural gas or hydrogen) can provide much higher storage capacities thanks to its intrinsic high energy density. Here the possibility of store large quantities of hydrogen which can provide, with its energy density of $\simeq 500^{kWh}/_{m^3}$(based on a pressure of 200bar and a temperature of 20°C), very large storage capacities. With a suitable storage facility it is then possible to store several hundreds of GWh of hydrogen chemical energy, which can be later reconverted into electricity or consumed as raw material to feed industrial, mobility or power to gas (P2G) applications. There are diverse challenges hydrogen must overcome: in order to use it to smooth power profiles, it must be economically sustainable and technically feasible to produce hydrogen from water electrolysis, exploiting RES variable electricity generation, meaning that hydrogen produced through electrolysis must be competitive with traditional hydrogen production technologies; compressed hydrogen in the form of above-ground tanks can be extremely expensive at the moment, so that underground hydrogen storage, possibly in the form of LRC, must be further studied and tested; finally it is important to understand what will be the driver of the hydrogen economy of the future and how and how much it will be interconnected with the power grid.

METHODOLOGY

The hydrogen storage system scheme considered for this study is represented in figure 1.

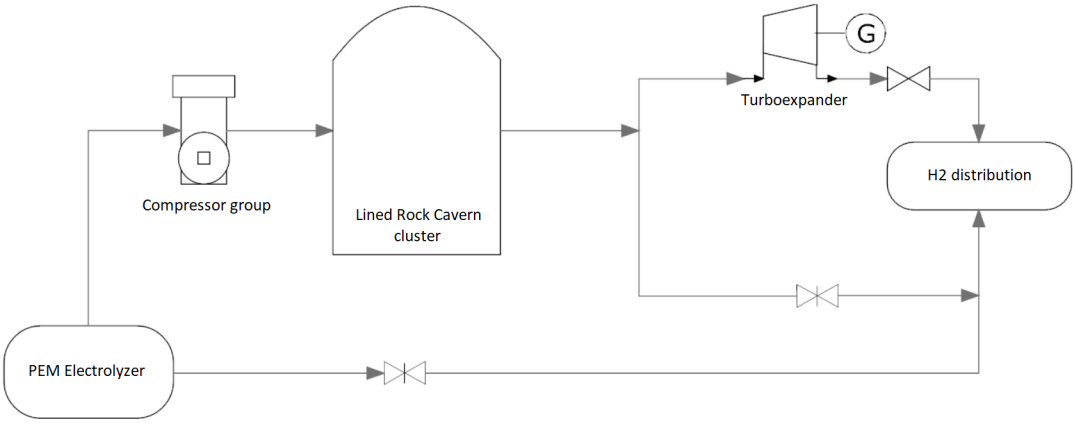

Figure 1: Storage system scheme

The Polymer Electrolyte Membrane (PEM), used to produce hydrogen from an electricity source, is not included in the model, but is important to understand the

choice of this particular technology. It has been shown that PEM electrolyzers can operate better than traditional alkaline electrolyzers when coupled with variable electricity generation. In particular they have a strong flexible operation in terms of load range, transient operation, cold/warm start-up and stand-by losses, so that they show lower losses of performance during discontinuous operation, when compared with the alkaline technologies, and can also benefit from intermittence in terms of recovery of the reversible parts of degradation processes. The hydrogen produced by the PEM electrolyzer is directly fed to the compression unit when the gas must be injected in the cavern, otherwise it is throttled to the final distribution pressure. The compressor is a well know reciprocating piston machine, commercially available for a wide range of pressure and flow applications. It is a multi-stage machine with inter-refrigeration stages needed to provide low gas discharging temperature, for wearing and safety reasons. Once the hydrogen is compressed it is injected into the lined cavern where it will exchange heat with the surrounding rock and through the metal and concrete liner of the cavern. When there is a hydrogen demand it is withdrew and expanded in a gas turboexpander to match the distribution pressure and partially recover energy; in particular if the cavern pressure is not high enough it is throttled to the final pressure. The cavern system is made of LRC with a double liner: a thin steel liner with the function of providing an impenetrable surface for hydrogen on the cavern walls and a 2 meters thick reinforced structural concrete liner able to smooth the load of the high-pressure gas, reducing the localized stress on the rock and the possibility of fractures. It is relevant to specify some characteristics and assumptions about the cavern: due to geo-mechanical reasons the cavern cannot be cycled too fast or too many times during a year of operation, meaning that there are constraint on the injection and withdrawal rates as well as on the maximum number of cycles during the year; moreover a minimum and maximum pressure are defined for each cavern respectively to avoid cavern convergence or liners and rock fractures. In order to take into account the operational constraints, the inlet and outlet maximum gas flows are limited and the inlet flow is further reduced according to a maximum number of yearly cycles: in particular this constraint is considered as a maximum yearly injection of gas and the single hourly injections are scaled down to accommodate it. The model has been coded in Matlab and the real gas properties of hydrogen have been used through the use of a Matlab library.

The model inputs are taken from the results of an cost optimization process of a European country national grid, produced by a GAMS model developed in the En-

ergy division of Chalmers University of Technology, which can provide both hydrogen production and demand patterns. Since the model is not optimized together with the production and consumption of hydrogen and due to the cavern operational constraints, there will be an excess of hydrogen production and a portion of the demand which will not be met and that will be considered as losses for the plant, since it will not be possible to store a portion of the already produced hydrogen or extract enough to fulfill the demand. However, since in a real plant operation it is not rational to produce hydrogen to waste it, the constraint on the maximum injection has been implemented in the GAMS model before the output was produced, so that in the described scenarios there will not be excess of hydrogen entering the storage plant. The model considers a year of operation with a 3 hours time-step. The injection section of the model has been studied with mass and energy balances in order to find the gas physical properties in the cavern after each injection step. The energy balance includes the heat exchange process between the injected gas and the surrounding rock with some main assumptions:

- rigid container
- perfect contact between steel, concrete and rock surfaces
- the surrounding rocks act as a constant temperature reservoir

which together with the hypothesis of negligible kinetic energy made possible to describe the heat exchange process by means of a lumped parameter representation, consisting in a conduction process through the two liners and a convective heat exchange between the gas and the internal cavern walls. The withdrawal process is described in analogy to the injection process, both in terms of mass and energy balances and heat exchange process. The simulation of the injection and withdrawal processes will define all the thermodynamic properties of the gas inside the cavern for every defined time-step. The compression process (shown in figure 2 for an arbitrary compression step) is described using hydrogen real gas properties and considering a real transformation through the definition of an isentropic efficiency; it is an inter-refrigerated compression with the number of stages depending on the maximum compression ratio, defined by the maximum cavern pressure.

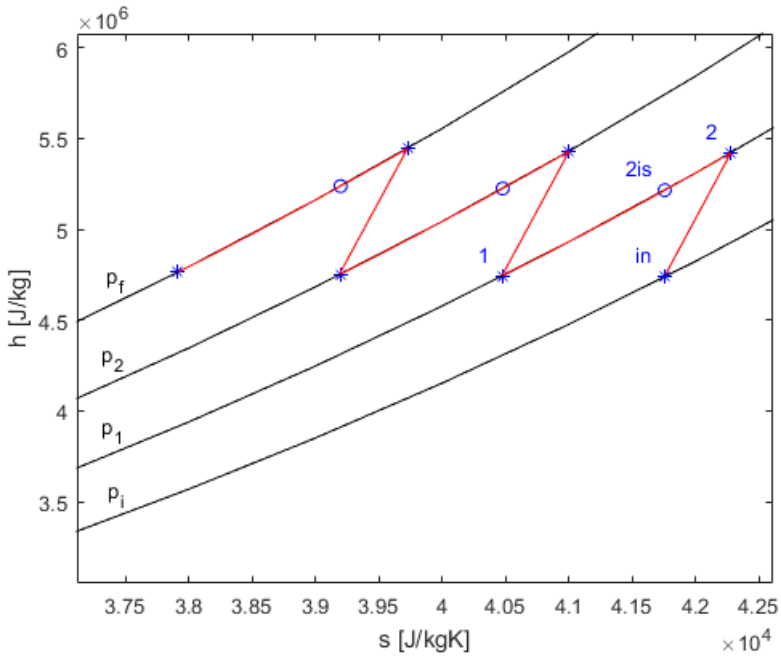

Figure 2: Compression process

In the same way it is possible to describe the expansion process, defining an isentropic expansion efficiency for the turboexpander. Once the operation of the cavern have been simulated for the considered year, it was possible to define some system performance parameters. In particular it was defined a system efficiency, which expresses how well the system performs in extracting most of the entering chemical energy during a year of operation. It will then be used, together with an electrolyzer and power unit efficiencies, to compare LRC storage with other electrical storage technologies. Once the thermodynamic behavior of the cavern has been defined, a system cost analysis follows. It is based on the definition of a Net Present Cost (NPC) with the following cost components:

- Compressor capital and O&M
- Cavern capital (including cushion gas)
- Turboexpander capital and O&M
- Excess of production and missed delivery

Compressor costs have been evaluated with the help of the tool *"H2A Delivery Components Model"*, while all the other assumed costs are based on literature benchmarking.

Excess of production and missed delivery costs are minimized (production excess in null) as already discussed in this same section. Once the NPC was defined, a delivery cost of hydrogen have been found and expressed in $\left[\$/\mathrm{kWh}_{\mathrm{H}_2}\right]$ or $[\$/\mathrm{kg}]$, which gives an idea of how LRC storage system can compete with different hydrogen storage technologies. Moreover an additional cost component have been considered in the NPC definition for a better comparison of the storage system with others electrical storage technologies or mobility applications: electrolyzing costs have been added assuming that the inlet hydrogen in storage plant has a fixed price (on a mass basis); finally a hydrogen-to-electricity conversion efficiency of 62% has been considered, assuming that the power unit is already available and does not contribute to the system cost. An electricity delivery cost expressed in $\$/\mathrm{kWh}_{\mathrm{el}}$has been found and discussed.

RESULTS

The aim of this work was the definition of the operational parameters of a LRC storage system in terms of gas flows, performances, maximum pressure and physical parameters variation during operation, as well as a cost analysis of the whole system to show potential and limits of the technology. Diverse cavern configurations in terms of shape, depth and volume have been fed to the model in order to find the most cost effective coupling among compressor unit, cavern and expander. Also four different hydrogen production and consumption patterns have been considered to produce more consistent results. In particular the installation of an expander was considered as a separate case, since the possible energy recovery did not justify its cost in every considered scenario.

The thermodynamic analysis shows pressure, density and temperature trends inside the caverns: here it is relevant to understand how the operation can change when considering, or not, the installation of the turboexpander. In particular, since the expansion process can benefit from high temperature inlet gas coming from the caverns, the gas from the compressor unit is not cooled down before its injection in the cavern, allowing a recovery of $7-10\%$ of the electricity spent for compression and pumping. This design choice will lead to a higher mean temperature in the storage, as it can be seen from figure 3, allowing $4-5\%$ less total hydrogen mass to be stored. This will not only influence the storage capacity but also boost, in most of the scenarios, its gas deliverability. The latter is indeed increased since, considering the same cavern volume, a higher temperature will lead to a higher pressure inside the storage, allowing withdrawals when operating in the range of pressure close to the minimum one, when it would not be possible to extract gas in the case without expander (the cavern pressure

would otherwise go below the minimum treshold).

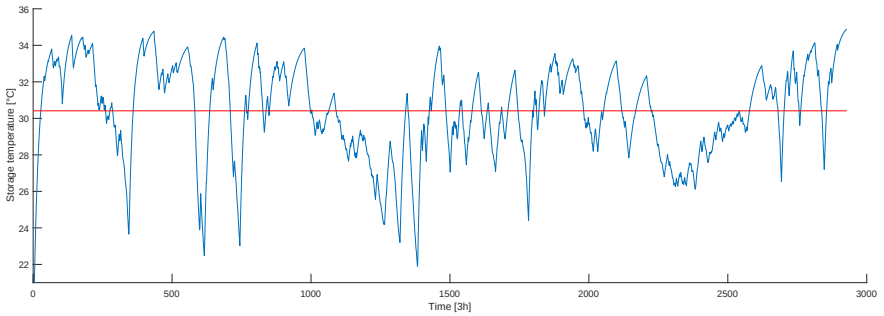

(a) T-t diagram expander case

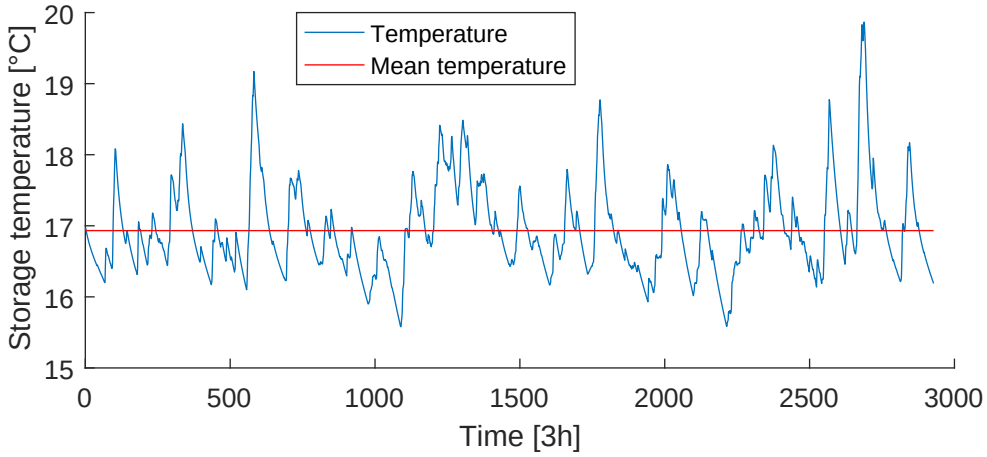

(b) T-t diagram w/o expander

Figure 3: Temperature trend inside the caverns

However $4-10\%$ of the total demand cannot be met for every year of operation in the different scenarios due to cavern technical constraints, concluding that an optimization process including also the electrolysis plant would be beneficial for the overall system operation and cost. The storage efficiency, defined as the capability of delivering most of the hydrogen chemical energy at the cavern outlet, ranges between $97-98\%$. It is reasonable to have low losses with the design choices of this study. In particular mass losses are only supposed to happen in the compressing unit (they account for 0.5% of the total mass flow rate); the compressor power consumption is limited since the gas must be compressed from an already high starting pressure of 30bar (outlet pressure of the electrolyzer unit) to a relatively low maximum pressure of $100-200$bar.

The cost analysis includes the main system components: compressor, caverns and

expander. Here the purpose was to understand if LRC storage could be competitive with other hydrogen technologies or electric storage alternatives. The main results are given in terms of delivery cost of hydrogen from the storage system, ranging between $0.009 - 0.015\,[\$/\text{kWh}]$ or $0.29 - 0.51\,[\$/\text{kg}]$ for the analyzed scenarios. These results have been obtained considering a cavern cyclability of 12 full charge-discharge cycles; according to found costs, LRC storage could be competitive with its alternative technologies, with the exception of tank storage, which cost could be as low as $0.17\,[\$/\text{kg}]$ if tanks are cycled at their maximum capabilities. Thus the cost is strongly influenced by the operation of the plant and must be evaluated for the particular scenario.

Capital cost distribution on an yearly basis is shown in figure 4, where it is easy to see how the cavern excavation could have an impact of more than 90% of the total investment cost.

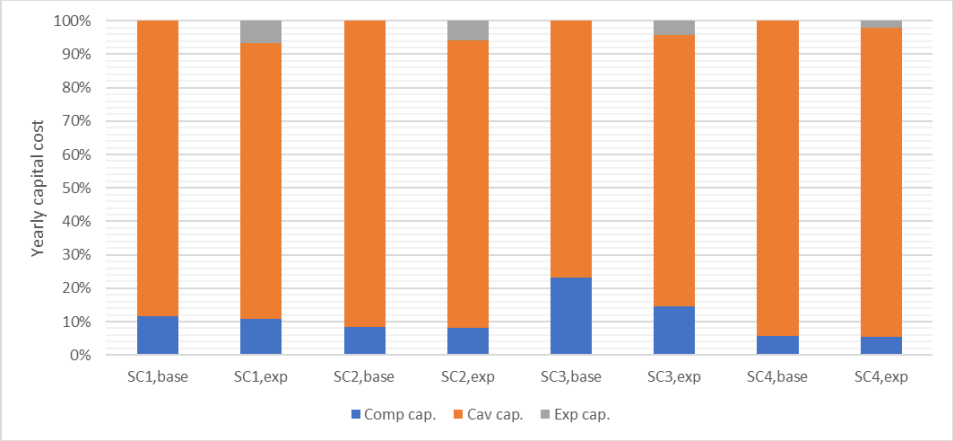

Figure 4: Yearly capital investment

However, considering also O&M costs as shown in figure 5, compressor O&M can be as high as cavern capital cost in particular scenarios. In particular O&M compressor cost are dominated by the electricity component, amounting to $75 - 77\%$ of the the total compressor O&M cost; in an system optimization logic these costs could be reduced, optimizing hydrogen production together to its compression to better exploit the market electricity price arbitrage.

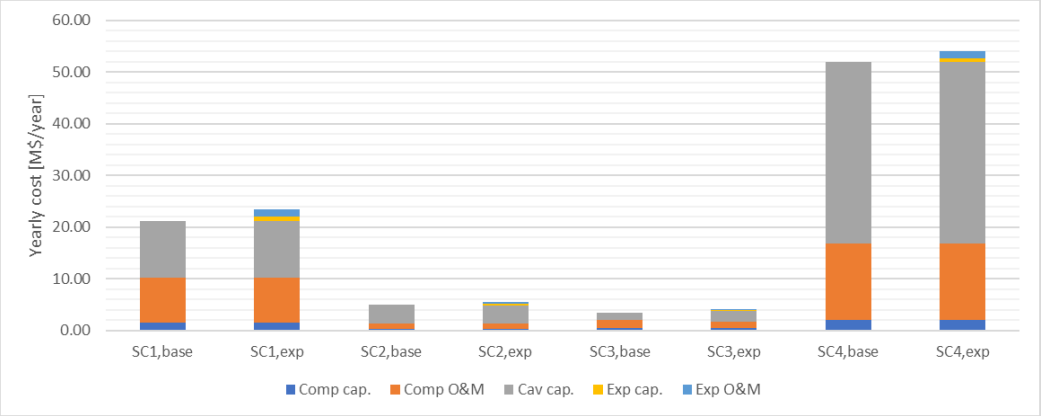

Figure 5: Yearly costs LRC plant

The comparison of LRC storage with electric storage has shown an electricity delivery cost of $0.26 - 0.27\,[\$/\mathrm{kWh_{el}}]$ based on actual prices of PEM electrolyzers, while a cost of $0.22 - 0.23\,[\$/\mathrm{kWh_{el}}]$ for PEM costs of 2025. The results are consistent with literature findings: hydrogen is actually economically competitive with most of the battery applications, but it is not with PHS and CAES. Only the possibility of exploiting very low electricity prices could lead to sustainable, grid connected, hydrogen storage systems. Finally a broad analysis of the impact of hydrogen on possible future electricity generation scenarios has been developed. It shows how hydrogen storage could become competitive in future scenarios characterized by the development of a market for raw hydrogen or a ban of electricity generation technologies involving biomass use. In most of the analyzed scenarios, employing hydrogen as storage, LRC had the largest capacity among the other storage technologies, showing a seasonal exploitation of the technology. However it was often coupled with more flexible storage choices as VRF batteries and tank hydrogen storage, in order to respond to fast fluctuations on the power grid.

Contents

Chapter 1

Introduction

The extensive utilization of hydrocarbon based technologies in the power sector accounts for 40% of the total energy related emissions and 25% of the total greenhouse gases (GHG) emissions [1, 2]. This led to a temperature increase of 0.8°Cin the last 120 year and could lead to a further increase of $2-6$°C by 2100, if no corrective actions will be applied [3]. The solution to the global warming problem will be a combination of increased energy efficiency, carbon capture and storage (CCS), biomass exploitation and renewable energy sources (RES) development. In particular RES have seen a strong expansion in the last 10 years, showing a growth of 22% and 46% per year for wind and solar respectively [4], the two technologies that are seen as the most promising for the future development of RES [1]. However RES suffer from strong disadvantages: fluctuation over time and not uniform spatial distribution, together with low capacity factors and uncertainty of the production predictions make their development constrained by a heavy utilization of flexibility measures. It is thus important to develop flexibility tools that are sustainable both from an environmental and an economical point of view. Flexibility is referred as the ability of the system to respond to events that can jeopardize its normal operation, no more providing the fundamental services to the end users [1]. It results that the system has to be able to cope with every variability source through the use of different flexibility options as network expansion, demand-side and supply-side management, curtailment or storage.

While several studies claim that grid management by electricity grid extension will render large-scale storage unnecessary, numerous studies estimate grid investment in the order of magnitude of tens of thousands of kilometers [1, 5] since the little significance, in terms of increased flexibility, in increasing long-distance transmission beyond the existing capacity [6]. Demand-side management is intended as an active response to end-user consumption and is very limited to those energy intensive industrial processes, shifting their peak consumption to base load hours. Supply-side management will be even more difficult to be applied in a future where most of the electricity is produced from unpredictable energy sources. Curtailment is also considered as a flexibility option, but it must be limited in order to avoid oversizing of power plants which could lead to increased capital costs. Storage is already being used as flexibility measure, but no application are still available to respond to seasonal variability. As it will be discussed in the following, storage could be one important flexibility option in a system with large shares of RES. Thus a combination of all the flexibility measures, with a particular focus on energy storage, will be necessary to achieve a high RES penetration with low technical, environmental and social costs [6]. In particular storage

can be applied to solve the temporal mismatch between generation and demand, from very small to large scale.

There are two main reasons to store electricity: to provide a less intermittent power generation from renewable; to exploit curtailed power or surplus supply in general, which is reflected in lower electricity prices. Storage technologies differ a lot each other both in terms of energy and power capacities, making impossible to refer to storage as a single flexibility measure. It is then possible to differentiate the storage role depending on the scale of the temporal fluctuation it is able to act on:

- Power quality
- Distributed generation
- Bulk storage
- Seasonal variability

Take as reference figure 1.1.

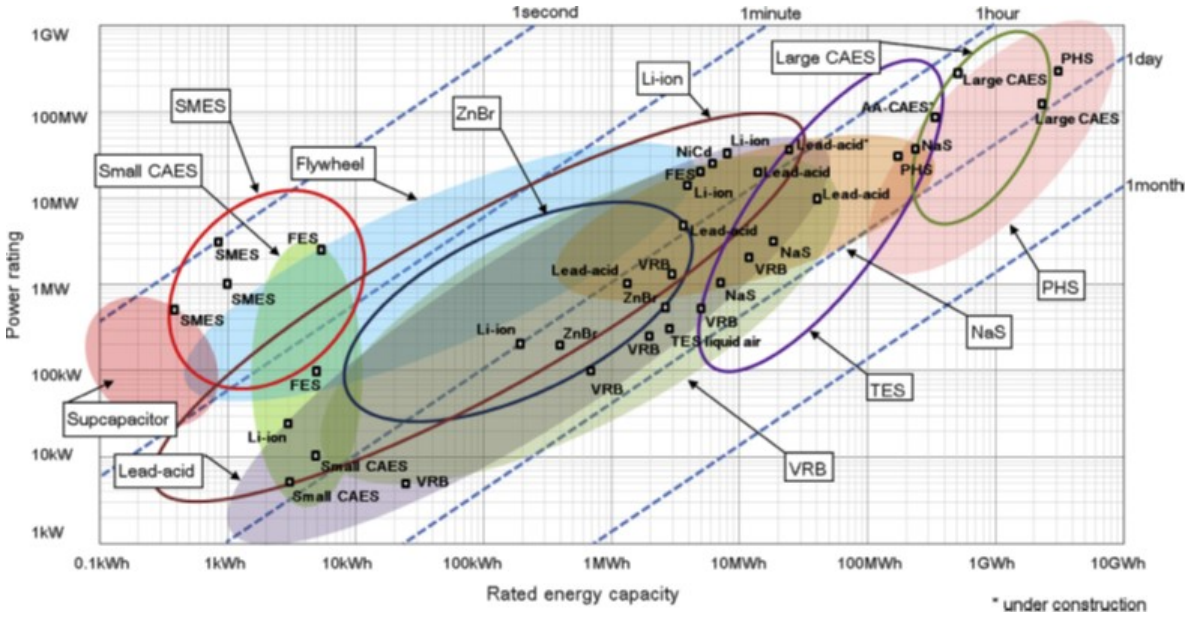

Figure 1.1: Storage scale [7]

Power quality applications require a very fast response from the storage, in the scale of msto s, so that the most common storage options are Lead-Acid and Li-ion batteries, flywheels, supercapacitors and SMES (Superconductive Magnetic Energy Storage).

These technologies can provide a short discharge time with a limited power rating, without having to provide large capacities, not required for power quality purposes.

Distributed generation storage, applied for peak shaving or transmission deferral, usually requires a time scale of min to hours, so flywheels could be adopted as well as diverse battery technologies and hydrogen fuel cells and engines, since they can provide relatively fast discharge time.

Bulk storage and seasonal variability refer to a time scale in the order of hours to months and it is possible to find application of the same technology for very different purposes. Technologies used for this application mainly focus on the energy capacity, since required power and discharge times are usually lower. While CAES can provide a power rating up to several hundreds of MW, PHS are the largest scale energy storage application that is possible to find. In particular they can provide energy storage up to several weeks if a moderate power rating is required. No technologies are available for a storage dimension above the the time span of a month, and no practical application of PHS are in use for storage times of more than one week [8].

One technology now under development is P2G, intended as the practice of producing hydrogen through a water electrolysis process, exploiting cheap electricity availability and eventually converting it in methane with the addition of CO_2. In particular electrolysis is a electro-chemical conversion of electricity into H_2, in which water is split by an electric current in H_2 and O_2. The development of P2G is controversial and its potential is only expressed in high RES penetration scenarios with extended focus on the future gas demand [1, 9] . Depending on the future storage scale requirements, on the development of integrated hydrogen markets and an integration of power and gas systems, P2G could represent a promising alternative within the energy storage technologies. Hydrogen offers some advantages over other existing technologies. When compared with other electricity storage options, hydrogen-based storage is very versatile, as it will discuss in section 1.1; it has high energy density which can provide long term electricity storage; it is independent on the location, so that it can be directly applied to leverage power plants or solve congestion nodes. Hydrogen can be directly used to power fuel cells for electricity production and transportation or as industrial raw material: the latter represent 90% of the total demand as it is an established market. Hydrogen demand for transportation is still below 1%, but several studies show its potential in future scenarios where “green hydrogen” is required: H_2 vehicles penetration could reach $9\% - 13\%$ of the total fleet by 2030 [10]. On the other hand, reconversion of hydrogen into electricity suffers from very high costs and

low roundtrip efficiencies (AC-to-AC), ranging from 20% to 48% at most [11], when compared with other energy storage solutions [12, 13]. Moreover it can be blended with natural gas for heat production or even for utilization in compressed natural gas vehicles [11].

It is also important to make a distinction between the potentials of using hydrogen as carrier and its later conversion into methane. In the latter case, methane has an already existing infrastructure and more knowledge (resulting in lower costs) of the power production processes. It can be injected in the gas grid or used as fuel to power gas turbines for electricity production purposes: some studies show how P2G, with methanation, can have a huge impact on future scenarios with 100% RES penetration [14, 15, 16]. In particular it is shown as P2G could affect every aspect of the future gas and electricity grid, decreasing the need for seasonal storage [14], decreasing costs for the gas grid [17] and how the absence of a P2G technology portfolio could lead to an increase of the system cost [18, 15].

1.1 Hydrogen storage

Hydrogen is an attracting energy carrier, since it makes possible to store large amounts of energy, it is CO_2 clean when burned, and it is easier to store when compared with electricity storage options. As already discussed, it can be produced from water electrolysis, requiring water and electricity as raw materials; it is an energy intensive process, thus the need of large availability of electricity. The focus of most of the studies found in literature is on the integration of electrolysis with renewable sources, in particular wind and photovoltaic (PV) plants; hydrogen produced from electrolysis can be later reconverted into electricity through the use of a power unit or directly exploited. There are two main alternatives to produce electricity using hydrogen as fuel: gas turbines or fuel cells. The former are conventional natural gas turbines, which can sustain blends of hydrogen in the fuel with only minor performance reduction in terms of efficiency and emission [19]. They can also exploit the O_2 produced during the electrolysis process in order to have a cleaner combustion, which cannot happen in fuel cells operation. However fuel cells can achieve higher efficiencies together with no CO_2 emissions, but at the price of very high investment costs [20, 21]. Due to the low roundtrip efficiency, it could be possible in the future to directly exploit the produced hydrogen in many different ways, once proper markets will be developed, as it will be discussed in section 2.6. However there are already available technologies to

produce hydrogen in large scale and with competitive costs. As it is shown in figure 1.2, where cost values are taken from [22, 23], traditional H_2 production technologies as steam methane reforming (SMR), coal gasification (CG) or auto-thermal reforming (ATR) are cheaper when compared with electrolysis from renewable sources.

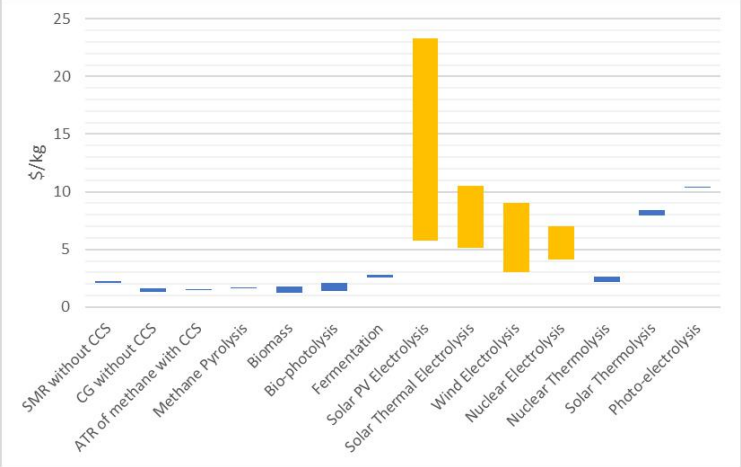

Figure 1.2: Hydrogen production cost

However it is important to clarify that costs found for electrolysis always include the cost of the electricity spent to power the electrolyzer. The actual electrolysis production cost depends on the operation and configuration of the plant, as well as on the electricity prices in a particular region or period. Moreover it must be noticed that electricity is the most important cost component in electrolysis H_2 production, as it is shown in [24]. Removing the electricity cost component, that is

$$\begin{aligned} \text{Cost reduction} &= \text{specific electricity consumption} \cdot \text{electricity cost} \\ &= 57\,[\text{kWh}/\text{kg}]\,34\,[\$/\text{MWh}] \cong 2\$/\text{kg} \end{aligned} \tag{1.1}$$

where the *electricity consumption* of the electrolyzer is taken from [25] and the price is referred to the average price of the US wholesale market in 2017 [26], the resulting production cost halves, becoming competitive with traditional technologies. However discontinuous operation should reduce the final production cost, enabling the arbitrage of grid electricity price variation; moreover decentralized production cost is only slightly higher (5%) than centralized production, so that it can already compete with traditional technologies for those applications [11].

Once hydrogen production from renewable power is found to be sustainable, it is important to compare hydrogen technology (production and storage) with its alter-

natives. It is difficult to show the potential of P2G when comparing it to electricity storage. In particular this comparison must be done in terms of electricity production, otherwise it would be impossible to compare different storage options. However when considering hydrogen storage, the fuel cell unit contribute to almost the 60% of the total investment cost, as it is shown in [24], making the following comparison only suitable in a scenario when hydrogen is used to produce electricity to feed the grid. Figure 1.3 shows the mid-range costs of electricity delivered from different storage technologies. It is then possible to see how hydrogen suffers from high conversion costs when compared with PHS and CAES, making it comparable with batteries in terms of costs. However a more recent study has shown as hydrogen storage costs are lower with respect to batteries in different scenarios [24].

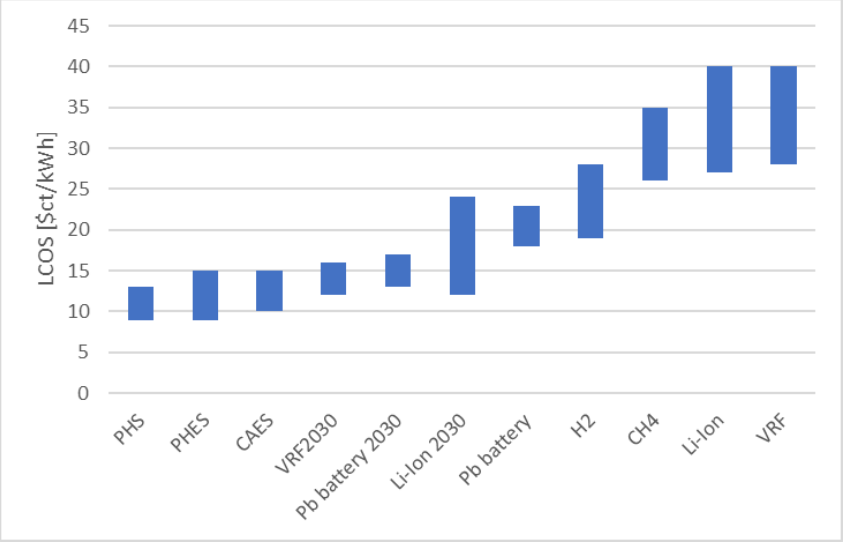

Figure 1.3: Electricity storage cost [12, 27, 28]

Going more in depth with the large scale hydrogen storage technologies, figure 1.4 shows the specific cost of storage for different hydrogen technologies.

Most of the technologies costs are estimations based on CO_2 and natural gas applications, with the exception of salt caverns and tanks; moreover it is important to point out that costs are referred to the working gas capacity of the storage. In particular hydrogen storage technologies differ each other in terms of cycling capabilities, showing very different costs when referred to the delivered amount of hydrogen. Depleted reservoirs and aquifers can only be cycled once per year due to the very slow injection and withdrawal rates, required to maintain the pressure inside the storage. Tanks can be cycled very fast and several times per day, since they can be charged and dis-

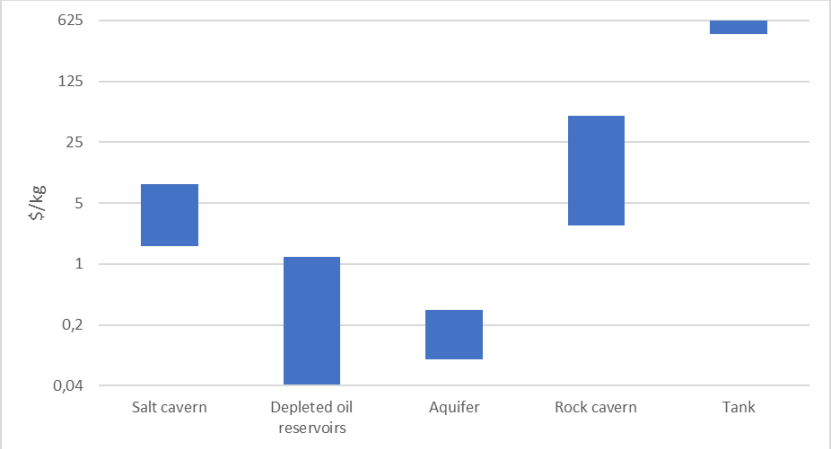

Figure 1.4: Hydrogen storage cost [24, 29, 5, 30]

charged in the time order of hours. Rock and salt caverns can be cycled several times per year, offering in this way not only a higher overall capacity, but lower specific cost per hydrogen withdrew. Finally the effective cost of hydrogen delivery from a storage facility will depend on the particular system, leading to specific delivery hydrogen costs in the range of $0.17 - 0.33 \$/kg$, where the lower region of the range is occupied by tank storage [29, 5].

Finally many conditions are necessary to see the development of hydrogen storage as a large scale application for RES electricity integration. Cost reduction must be applied to components that more influence the final cost of hydrogen/electricity production, in particular electrolyzers and fuel cells. However the cost trend of the PEM electrolyzers seems to point to a further reduction in the near future, since it has already dropped from $3400 \$/kW$ to $1600 \$/kW$ from 2012 to 2017 and it is expected to further reduce to $900 \$/kW$ and $700 \$/kW$ respectively by 2020 and 2023 [25, 31]; in the same way fuel cell have seen heavy reduction of the cost in the last years and the manufacturing cost is supposed to be further reduced [32]. Hydrogen storage must be chosen as a valid flexibility option, moving investments from other technologies or applications in order to help with the cost reduction process. Moreover the hydrogen economy development will be strictly connected with the RES penetration since it can heavily benefit from a highly variable electricity production and cost and eventually replace curtailment employment. As it will be discussed in 2.6, power and heat sector integration and the development of a mobility market for hydrogen could increase its demand and then contribute to development of the production and storage technologies, upstaging fuel cells electricity production.

Chapter 2

Technologies

It will follow an overview of the most relevant technologies for large-scale electricity storage, with a particular focus on hydrogen storage applications. These technology descriptions include information on system design, performance and technical maturity.

2.1 CAES

Compressed air energy storage systems have three main components: an air compressor driven by a motor; an underground storage, such a salt dome, a cavern or an aquifer; a combustion turbine that drives a generator. They have some attractive qualities in terms of operation, as their quick start-up ($9-12$ minutes), long storage period (over a year) and relatively high efficiencies ($50-70\%$) [33]. Figure 2.1 shows the layout of a CAES plant. The motor driven compressor is operated during off-peak hours,

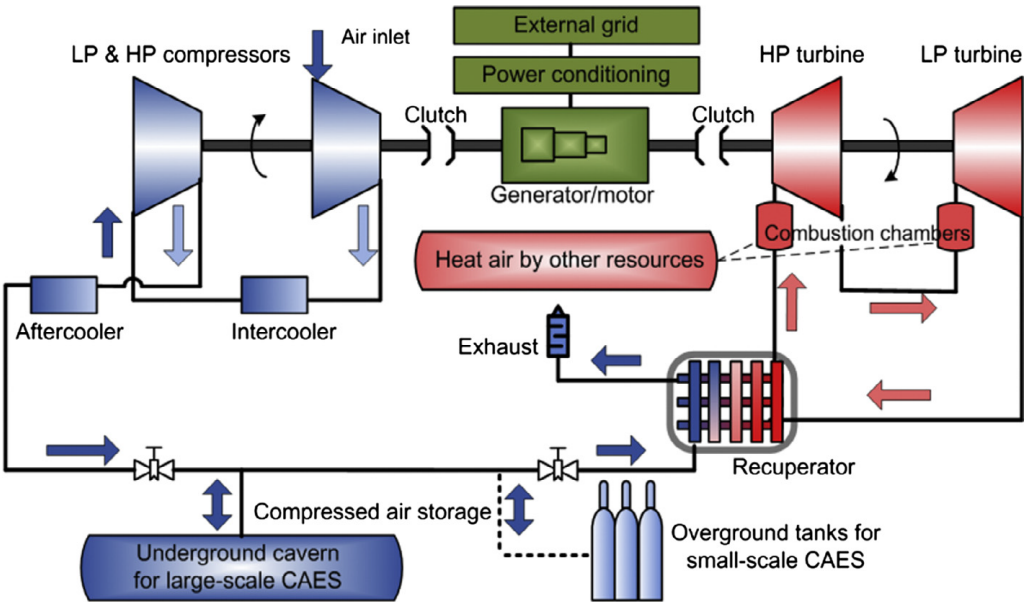

Figure 2.1: CAES layout [7]

in order to increase the air pressure inside the storage. During high demand periods the turbine is operated to expand the high pressure air coming from the storage. The air is firstly preheated in a recuperator and expanded in an air turbine and eventually mixed with natural gas, burned in a combustor and expanded in a gas turbine, in order to further increase its temperature and achieving higher turbine efficiencies. Even if it is a mature technology, there are only two operational CAES plants worldwide, a 321MWe at Huntorf in Germany and a smaller 110MWe at McIntosh in USA; several

plants are planned or under development. Different plant configuration can be tested based on the aim of the project: Advanced Adiabatic CAES (AA-CAES) integrates a thermal storage to avoid fuel combustion to increase the air temperature before expanding it in the turbine, so to have a CO_2 free final system; otherwise, to achieve a CO_2 free storage operation, it is possible to avoid the combustion before and after the first expansion stage (figure 2.1), loosing performances in terms of system efficiency. CAES can also be more efficient and environmentally friendly than PHS, but it can be difficult to find a suitable site and they have a long construction time and a high initial cost. Moreover relatively low roundtrip efficiencies have been shown in the only two operational plants (respectively 42% and 54% for Huntorf and McIntosh) in comparison with battery storage or PHS [7]. CAES plants could be a more interesting storage option if coupled with a wind farm, able to provide cheap electricity to compress the air, since the electricity delivery costs of CAES plants are dominated by the cost of electricity used to drive the compressor. Moreover, when considering a thermal storage as design choice to avoid fuel burning in the gas turbine, it would be possible to exploit the cost reduction due to CO_2 taxation to compensate for lower CO_2 emissions, reducing the specific storage costs by 10% [34]. When directly compared with underground hydrogen storage, which will be analyzed in detail in section 2.4, CAES result in a lower capital cost and a more mature technology for the power production unit; however it cannot provide the same storage capacity as hydrogen application, making a direct comparison irrelevant if considering the same storage necessities.

2.2 PHS

Pumped hydroelectric energy storage is based on conventional hydroelectric technologies. Its use consist in storing excess electricity from coal-fired or nuclear plants at night, when electricity is cheaper, using it to power water pumps able to move large volumes of liquid in the higher reservoir (figure 2.2). During peak hours the water is released back into the lower reservoir: during this process the water drives a turbine unit which powers the electrical machine to generate electricity. There are two main types of PHS facilities: *pure* or *closed-loop* PHS which only rely on the water previously pumped in an upper reservoir as source of energy; *combined* PHS which use both pumped and natural water streams to generate power.

PHS is the only widely adopted utility-scale electricity storage technology with a worldwide installed power capacity of 168GW[36]. There are several existing plants

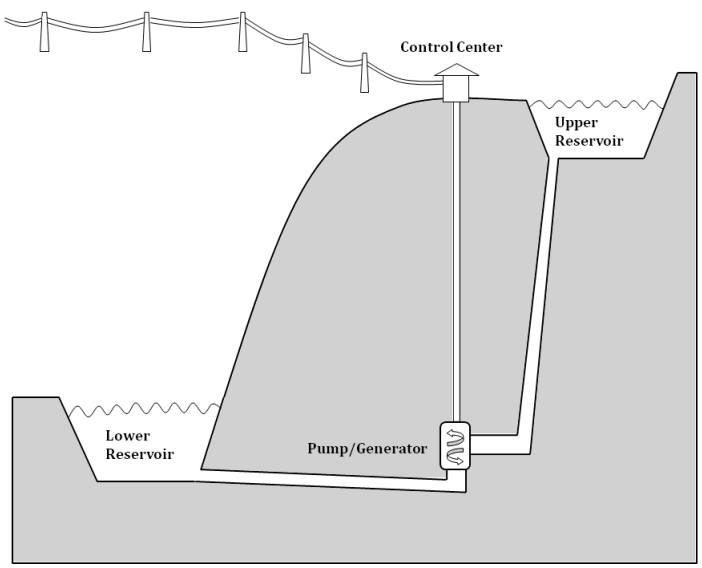

Figure 2.2: Pumped hydroelectric storage plant layout [35]

with power ratings ranging from 1MW to 3GW with high roundtrip efficiencies in the range of $70-85\%$ [7]. They can be used for energy-balancing, stability and ancillary grid services such as network frequency control and reserves since they can respond to electrical load changes within seconds. The most important use for PHS has traditionally been to balance base-load power plants, but in the last years wind and solar power generation coupled with PHS is being developed: this could help both with isolated and distributed networks.

However there are several drawbacks in PHS technologies. Due to the low energy density of these systems, to produce reasonable amounts of energy for bulk energy storage PHS plants need very large installations and large height difference between the upper and lower reservoirs, with consequent considerable planning as well as environmental permits. Due to its intrinsic nature, PHS finds only few suitable sites where adequate conditions are met for the construction of the plant: in particular it is hard to find adequate water flows and upper and lower reservoirs positioning [37]. Conventional PHS construction can involve damming a river and this could hardly influence the terrestrial wildlife as well as changing the landscape. Moreover the water temperature is increased due to pumps operation, deteriorating the river water habitat. The construction time of PHS plants can be as high as a decade and, even if the operation and maintenance cost is very low, they suffer of high upfront capital investment, only recovered over decades [35].

2.3 Batteries

Batteries are a form of electrical energy storage technology characterized by high modularity, rapid response and a high commercialization potential. In the last years they have seen strong improvements in efficiency, energy and power density, cycle life. Together with their flexible installation and short construction periods, they are a strong alternative for grid energy storage applications, still limited in terms of installed capacity (2GW worldwide in 2016) but rapidly growing. Only three technologies are actually mature for grid support, which will be described in the following sections, while others are under development, as Nickel-Cadmium and Sodium Sulfur Batteries. A typical battery storage system is composed by a battery pack, battery management system (BMS), power conditioning system (PCS) and energy management system (EMS). The BMS monitors battery's parameters and control the overall system; the PCS manages the inversion and rectification for the AC-DC conversion; the EMS is responsible of the connection between the storage system and the grid [38]. Several battery technologies are available for grid support storage applications, but only the most relevant will be discusses.

Lead-Acid Batteries

Lead-acid or Pb-acid batteries use lead and its oxide as electrodes and a sulfuric acid solution as the electrolyte. Lead-acid batteries are used today in several large installations. The main cost component for this technologies is the balance of plant, related to the building of constructions, battery installation, interconnections, heating, ventilating and air conditioning systems etc. Their AC-AC efficiency is in the range of $70-80\%$ depending on operating conditions. Despite the very high upfront investment, they have very low O&M costs if replaced every 6 years, typical lifetime of this technology; moreover they are the most mature technology with the lower cost among battery technologies. However they have poor performances when fast discharge is needed, showing low energy and power densities, long charge time, high self-discharge rates and finally environmental pollution problems, which is limiting their installation in the power grid. There are some variation of this technology which are being experimented in order to increase its cycle life, in particular ultrabatteries and advanced lead-acid batteries, which are both based on the addition of activated carbon into the electrode [39].

Vanadium Redox Flow Batteries (VRF)

VRF batteries are relatively mature flow batteries based on reduction-oxidation reactions with exchange of electrons between forms of vanadium. The main advantage of a flow battery is that it is possible to separate power and storage units, designing and sizing them based on the particular application. The electrical energy is stored in the form of chemical energy in the sulfuric acid electrolyte and the conversion between electric energy and chemical energy is driven by the change of the valence state of the vanadium ion contained in the electrolyte, which create an electrons flow during the battery operation. Their efficiency remains in the same range of lead-acid batteries, ranging between 70% and 85%. Vanadium batteries show predicted lifetime, for the electrolyte solution, of more than 50 years, with very little degradation of the electrolyte during operation and the possibility to recover or reuse the precious vanadium, helping to extremely reduce replacement costs, but they still suffer from high construction capital [12].

Lithium-ion Batteries (Li-ion)

Li-ion batteries are based on the movement of the lithium ions between positive and negative electrodes. While charging the battery, ions will move from the positive to negative electrodes, through the electrolyte; during discharge the opposite happens. Positive electrodes are composed by lithium based compounds, while the negative electrodes is usually made of graphite. Despite their very high energy efficiency of $90-94\%$ in comparison with other batteries, Li-ion technology suffers from very high initial capital cost, poor cyclability and short lifetime in the range of $5-15$years and safety issues related to overheating during overcharging, limiting its application in the power grid [39].

2.4 Hydrogen storage technologies

Hydrogen storage can be classified in:

- Physical storage as compressed gas
- Physical storage as cryogenic liquid
- Material based storage

Material-based storage in terms of adsorption and absorption is not considered a valuable option for stationary applications mainly due to the high specific cost per kWh of storage [30]. Liquefied hydrogen storage tends to be very costly due to the losses in the liquefaction process: hydrogen must be cooled down to 21K loosing around 30% of its Lower Heating Value (LHV) energy, which is double the energy needed for compression alone. Moreover, due to the boiling process inside the container, $2-3\%$ of the hydrogen energy is lost per day with evaporation. Large-scale storage differs from vehicular or bulk transportation storage due to the lower restrictions in terms of dimension and weight, since the need to fit the storage vessels in vehicles or to avoid high costs for deliveries [30]. There are many reasons to assume compressed gas storage as the sole alternative to large-scale storage:

- Lower cost per kWh with respect to the alternatives
- Reduced complexity of operation and losses
- Possibilities to reach high storage capacity with a further reduction of price

2.4.1 Compressed gas technologies

When it comes to store compressed gas, it can be achieved in several ways:

1. Tanks
2. Buried pipelines
3. Salt caverns
4. Underground
5. Abandoned mines
6. Underground caverns

The most spread way to store hydrogen for medium-scale applications is based on above-ground cylindrical tanks. They have high dynamism in terms of cycling, up to 150 full charge-discharge cycles per year and this is the reason why they are used mostly in chemical industry, where hydrogen production and consumption is variable in the very short term. Pipelines storage is a powerful alternative when the land usage can be a problem or if a hydrogen distribution infrastructure is needed. However

these two technologies suffer from high specific costs, especially when it comes to have a less dynamic storage [5]. There are many applications worldwide showing the possibility to store hydrogen inside artificial underground salt caverns. They can store hydrogen up to 220bar and above [40], thanks to the low permeability of salt formations, which makes the technology attractive if related to the high volume capacity of the existing caverns. Hydrogen can be extracted and injected at a much lower rate with respect to a tank, making this application suitable to accommodate monthly and seasonal fluctuation in hydrogen production and demand. Moreover the specific cost of salt cavern storage is around one order of magnitude lower than the tanks one [5]. However in regions where geological salt deposits are not available, the application of this storage option is impossible. Underground storage in the forms of aquifers, porous rock formations, abandoned or depleted oil&gas reservoirs have been investigated. The larger limitation of these storage forms is the lack of knowledge in terms of hydrogen reaction with minerals (for example sulfur), which could lead to contamination and losses; reaction with microorganisms which could block the pore space; contamination with residual hydrocarbons.

Abandoned mines need to be re-evaluated from a gas tightness point of view. Usually rock walls are fractured due to extraction stress and this poses a huge problem in term of gas leakages and no evidence of undergoing experimentation for hydrogen storage has been found.

Underground hard rock caverns are underground cavities mined with conventional techniques (shaft sinking, excavation of cavities by blasting or cutting). They must be gas tight in order to prevent leakages through the rock formation and the gas pressure must be maintained above a minimum value to avoid contamination from external flows (to avoid water entering in the cavern, the pressure must be maintained above the water column pressure). The maximum operating pressure within these cavern is limited since most of the rock are not entirely impervious. The rock formation has to be hard enough to tolerate the operating pressure without fracturing and this is one of the reasons why the application of this storage technology is limited to some geographical regions.

2.4.2 Lined Rock Cavern

It is possible to line the internal walls of a rock cavern by means of concrete and steel: these are referred as LRC and it is represented in figure 2.3. The only operative applica-

tion of a LRC is based on natural gas storage and it is located in Skallen, Sweden. The Skallen storage facility has a rock cover of 115m, a storage volume of $40,000\text{m}^3$ and a maximum operating pressure of 20MPa. LRC technology will be briefly introduced in the following sections.

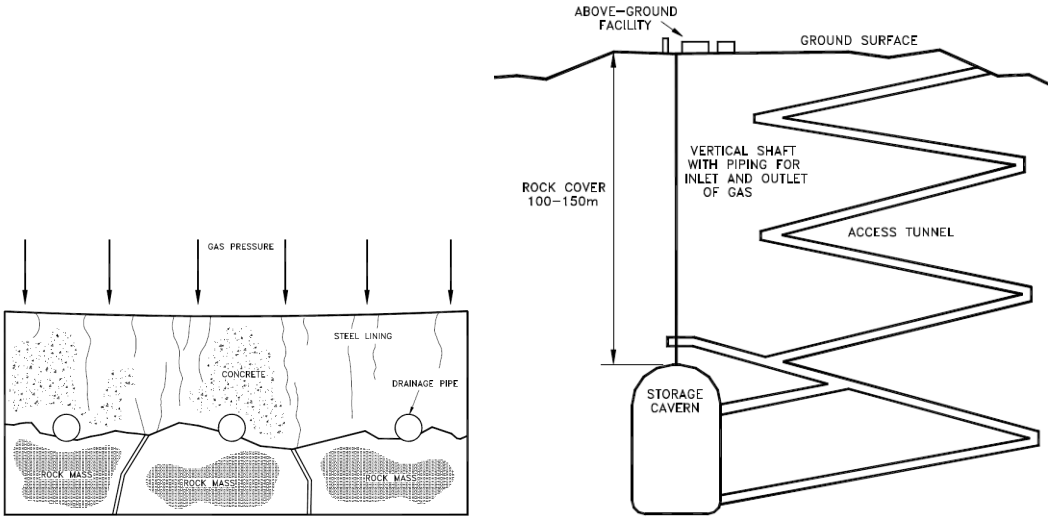

(a) LRC wall design (b) LRC underground section view

Figure 2.3: Lined rock cavern [41]

Liners choice and functions

With reference to figure 2.3a, a first thick reinforced concrete liner is applied to the cavern walls with the main functions of transferring the high pressure gas load to the surrounding rocks and providing a smoother surface for the application of the internal metal liner. The concrete layer will also be able to reduce the strain in the metal lining, which would be caused by the direct fracturing of the surrounding rocks [41].

The internal metal liner must be gas-tight and resistant to hydrogen corrosion. It should not be designed to bear mechanical loads (other than its own weight) since it supported by the concrete liner which is in turn supported by the surrounding rock. However it must be able to resist stresses and strains caused by the cyclic behavior of the cavern pressure which will cause elastic and also plastic deformation on the cavern walls. Plastic materials and steels have been studied, by the Geotechnical Engineering Department of the Chalmers Technological University of Gothenburg, for the application to the natural gas storage and it results that an austenitic steel is suitable since

it is ductile enough and has the ability to bridge over cracks formed in the concrete liner [41]. Since this study is based on hydrogen storage, it results that austenitic steels with a *Cr-Ni-Mo* are able to last for a service life of 40year for hydrogen tank storage applications [42].

Excavation

Feasibility analysis based on economical and geomechanical optimization processes consider a typical cavern design: a cylindrical shape with hemispherical top and bottom [43, 44, 45]. The excavation process can be divided into 4 main steps:

1. Access tunnel
2. Storage cavern
3. Shaft for gas pipes
4. Grouting and rock supporting operations

The tunnel excavation is based on conventional drill-blast methods, planned to minimize the amount of excavated rock and it is dependent on the particular application. Tunnels must allow vehicle access, turning operation and meeting places, so that the horseshoe cross section is in the order of $25m^2$. Rock support and grouting will be used along all the excavation process of the tunnel, when needed. Every cavern will need the excavation of two shafts each containing the injection or extraction pipelines. Cavern excavation starts more traditionally from the top and proceeds downward, since the hemispherical roof excavation is one of the most critical step. A central shaft in the cylindrical region of the cavern can be used to dump the excavated rock to the lower part of the cavern, which must be also excavated from the lower entrance. The bottom of the cavern is excavated as last step, and usually the perfect hemispherical shape is replaced with a more flatter one since the significant problems encountered in shaping it.

Accessory components

A detail of the design of the cavern that must be taken into account is the drainage system: it is build inside the concrete lining and it is used to reduce the hydrostatic water pressure outside the cavern in order to avoid excessive loading on the liners from the outside (for example during low pressure operation for maintenance or inspection).

Moreover the installation of a gas re-circulation system could be considered if the operation simulation shows too high/low temperatures during extraction, static storage or withdrawal. Since in this study the temperature seems to remain in an acceptable range of variation [41], the re-circulation system will not be considered in the final design of the cavern.

Cavern operation

The cavern will always operate in variable thermodynamic conditions, within a range of pressure and temperature. The minimum and maximum pressures are defined by means of geomechanical and safety reasons. Minimum and maximum temperature could be defined respectively in order to avoid water freezing in the cavern surroundings and poor efficiency in term of heat losses and amount of mass stored. During the injection process the gas must be compressed at a pressure slightly higher than the storage one (in order to make the injection feasible and to overcome eventual pressure losses in the system, which for sake of simplicity are not considered in the model developed in this study) before entering the cavern. It is thus necessary to know the pressure inside the cavern from installed instrumentation. The withdrawal process consists in a direct flow from the cavern through a throttling valve or a turboexpander, reducing the gas pressure to the one defined by the distribution pipeline. It is also important to define a maximum number of full cavern charge-discharge cycles during the year due to reasons related to liner fatigue failure: in particular too fast cavern cycling could lead to an impairment of the cavern walls and eventually lead to the formation of fractures on the metal and concrete liners as well as in the surrounding rocks.

2.5 Water electrolysis technologies

A brief description of the electrolysis process and technologies will follow, with a particular attention to Polymer Electrolyte Membrane electrolyzers, since their particular ability to well match intermittent electricity sources. They can be classified on the basis of the applied electrolyte.

Water electrolysis is an electrochemical splitting of water into hydrogen and oxygen by a supply of electrical and thermal energy, where the the reaction is given by

$$H_2O \longrightarrow H_2 + \frac{1}{2}O_2 \tag{2.1}$$

The overall energy required by the reaction ΔH is supplied by heat (ΔQ) and electricity (ΔG)

$$\Delta H = \Delta G + \Delta Q \tag{2.2}$$

Without going into the detailed thermodynamic of the reaction, it is important to notice how the minimum electrical demand ΔG can be reduced increasing the operating temperature of the electrolyzer, increasing the share of heat integration : this mechanism is exploited by technologies able to operate at high temperature $(600 - 900°C)$ [25].

2.5.1 PEM electrolyzers

Polymer Electrolyte Membrane or Proton Exchange Membrane electrolyzers layout is described in figure 2.4.

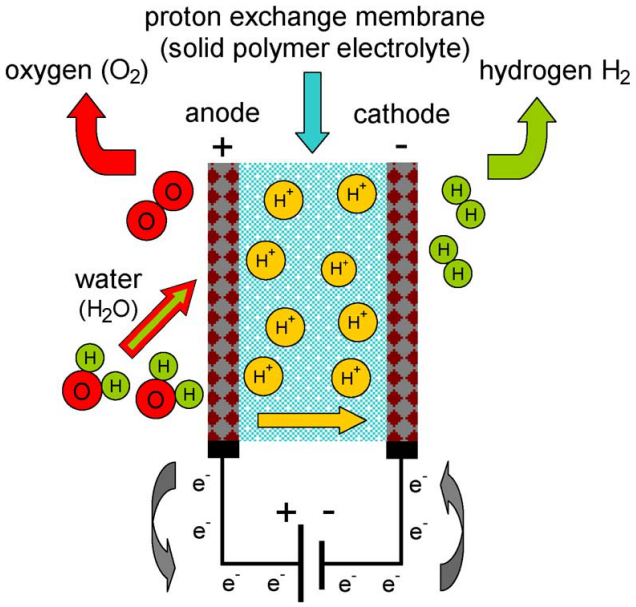

Figure 2.4: PEM electrolyzer layout [46]

A proton exchange membrane separates the two half-cells and the electrodes are mounted on the membrane. The electrolyte is a gas-tight polymeric membrane with a cross-linked structure. Due to the corrosive acidic regime provided by the membrane (presence of $-SO_3H$ groups), noble metal catalyst are necessary: iridium for the anode and platinum for cathode. Water is supplied at the anode where it is oxidized according to 2.3, to produce oxygen electrons and protons that are reduced at the cathode according to 2.4 to close the circuit and produce hydrogen bubbles towards the

cathodic manifold

$$H_2O\,(l) \rightarrow \frac{1}{2}O_2\,(g) + 2H^+\,(aq.) + 2e^- \tag{2.3}$$

$$2H^+\,(aq.) + 2e^- \rightarrow H_2\,(g) \tag{2.4}$$

Thanks to the very low permeation of the polymer electrolyte membrane, a high purity hydrogen is produced, with typical values higher than 99.99% after drying, up to 99.999%.

Moreover PEM electrolyzers are compact since the solid membrane application and can support high pressure hydrogen output since the high current density operation; moreover the compact nature of PEM leads to output pressure up to 85bar, reducing the power needed to further compress the gas for storage applications. In particular P2G applications require a strong operation flexibility which can be found in good performances in terms of load range, transient operation, cold/warm start-up (shorter heat-up times when compared with other technologies, thanks to the low heat capacity following from the compact design and lower operating temperatures) and stand-by losses; PEM electrolyzer are an attracting technology for P2G and it is easy to find studies focusing on their ability to well match RES, reducing their variability and achieving a stronger grid integration [47, 48, 49, 50], as there are several large-scale pilot plants for P2G application already in operation, showing the technical feasibility for flexible operation of PEM electrolyzers [25]. Table 2.1 shows these characteristics in comparison with other technologies.

The load range is very broad, meaning that PEM electrolyzers can be operated at almost every nominal load fraction, with some exceptions at very high pressures where there can be gas contamination issues. Electrolysis system can be operated dynamically and there are some applications and experimentation of PEM electrolyzer units to frequency regulation and grid balancing [25]; moreover intermittent operation can be beneficial as it causes reversible parts of degradation to recover [51].

2.5.2 Other technologies

Alkaline electrolysis (AEL) is the most mature available technology and it is already being used for large-scale hydrogen production. Electrolyzers show a relatively long life-time of 15 years when compared with PEM electrolyzers and they are reliable

	AEL	PEM	SOEL
Cell temperature (°C)	60–90	50–80	700–900
Typical pressure (bar)	10–30	20–50	1–15
Current density (A/cm2)	0.25–0.45	1.0–2.0	0.3–1.0
Load flexibility (% of nominal load)	20–100	0–100	−100/+100
Cold start-up time	1–2 h	5–10 min	hours
Warm start-up time	1–5 min	< 10 s	15 min
Nominal system efficiency (LHV)	51–60%	46–60%	76–81%
Specific energy consumption (kWh/Nm3)	5.0–5.9	5.0–6.5	3.7–3.9
Max. nominal power per stack (MW)	6	2	< 0.01
H2 production per stack (Nm3/h)	1400	400	< 10
Life time (kh)	55–120	60–100	8–20
Efficiency degradation (%/a)	0.25–1.5	0.5–2.5	3–50
Investment costs (€/kW)	800–1500	1400–2100	> 2000
Maintenance costs (% of investment costs per year)	2–3	3–5	n.a.

Table 2.1: Electrolyzers characteristics [25]

and safe. In the last years the efficiency has been improved through a reduction of the electricity consumption, circulating current densities have been reduced with a following reduction of the investment cost, together with some minor improvements on materials, chemistry and engineering of the cell. The operating principle is different with respect to PEM: water is fed at the cathode, where it is reduced according to 2.5 to produce hydrogen and hydroxide anions that circulate across the diaphragm to the anode, where they recombine according to 2.6 to produce bubbles of oxygen.

$$2H_2O\,(l) + 2e^- \rightarrow H_2\,(g) + 2OH^-\,(aq.) \tag{2.5}$$

$$2OH^-\,(aq.) \rightarrow \frac{1}{2}O_2\,(g) + 2e^- \tag{2.6}$$

One main problem of coupling alkaline electrolyzers with RES is that the production rate is limited to $25-100\%$ of the nominal range to prevent formation of flammable gas mixtures. Maximum electrolysis pressure are in the range of $25-30$bar, since the increase in the operating pressure triggers a strong increase in the investment costs for this technology, as well as the risks of formation of hazardous gas mixtures. Hydro-

gen purity is also lower (when compared with PEM and without auxiliary equipment) reaching value of 99.9% with the necessity of a very pure water feed, needed to let operate safely and protect the electrodes [46].

Solid oxide electrolyzers (SOEL) are based on steam electrolysis at high temperature ($600-900°C$), which results in higher efficiencies when compared with traditional technologies. Steam is fed at the cathode where water is reduced to produce hydrogen according to 2.7; the oxide anions pass through the solid electrolyte to the anode, where they recombine to form oxygen and hydrogen according to 2.8

$$H_2O(g) + 2e^- \rightarrow H_2(g) + O^{2-} \tag{2.7}$$

$$O^{2-} \rightarrow \frac{1}{2}O_2(g) + 2e^- \tag{2.8}$$

The attractive concept of this technology is that it requires less electricity for the splitting reaction since, as the temperature increases, more energy can be provided in the form of heat according to 2.2, so that it is possible to couple the electrolyzer with an available heat source as nuclear reactor heat or geo-thermal energy. However high temperatures imply also concerns in terms of thermal stability of the materials and the electrolyzer output is a mixture of steam and hydrogen which must be further processed. Currently solid oxide electrolyzers are at the R&D stage, so that they will require at least 10 more years to be commercially available, being the degradation of the involved materials the main obstacle to their deployment [46].

2.6 Hydrogen markets

An overview of the hydrogen market segmentation and the future prediction about its development will be discussed in this section. The largest share of the hydrogen market is occupied by industry, which represents more than 90% of the total consumption in Europe; the remaining 10% is shared between mobility and P2G applications.

Industry is the larger producer and consumer of hydrogen in Europe, where the main segments are chemical, refineries and metal processing, followed by sub-segments as aerospace, glass and food processing. The main chemical sub-segment is ammonia production which alone accounts for more 50% of the total hydrogen consumption; methanol accounts for the 12% of the market share, while polymer and resin production saturate the rest. Refineries represent the second largest consumer within the

industrial sector with a relative share of 30%. Metal processing is mainly referred to iron reduction and it represents 6% of the consumption. A graphical representation of the industrial sector share is proposed in figure 2.5.The industrial sector consumption is supposed to further grow at a rate of 3.5%per year at least up to the year 2025 [10].

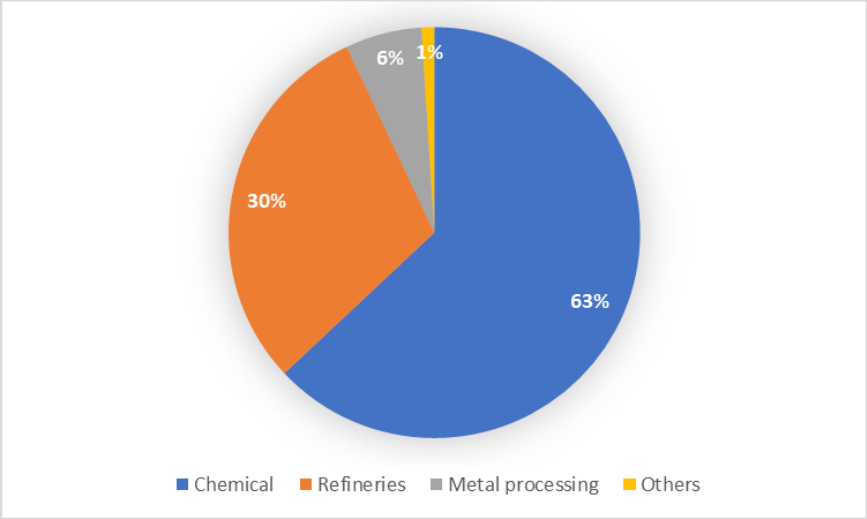

Figure 2.5: Industry market shares for hydrogen

In order to achieve the EU target on CO_2 emission reduction in 2050 the mobility sector needs 95% of decarbonization. Fuel cell vehicles (FCV) could have a huge impact on the emission reduction scenario and they are ready to be commercialized, but the lack of infrastructures and subsidies is slowing down its development. Thus the hydrogen demand from the *mobility* sector is today limited to a few demonstration project throughout Europe and thus its demand is today almost negligible. However a number of studies have shown market outlooks for impact and dimension of the penetration of FCV in Europe. According to [10], in 2025 the FCV fleet could reach a penetration rate of the 3% in a high policy support, modest learning scenario, while a 7% in a high policy, fast learning scenario reaching a $9-13\%$ of penetration by 2030. Moreover a study from McKinsey has estimated a number of 2300 retail stations already in 2025 with 25% of FCV penetration, reaching 5100 stations in 2030 [52]. Looking a the ultimate 2050 target, [10] shows a penetration of 35% for a modest policy, modest learning scenario up to more than 70% in the best case scenario, while according to [53] it will amount to 30% of passengers cars vehicles. According to [5] the only future hydrogen market with positive margin (with hydrogen produced from water electrolysis), with an outlook to the 2025 and 2050, is the mobility sector which in turn will not be sustainable in the case of high future electricity costs. Thus the mobility sector probably

will be the main driver for the hydrogen economy development, both in term of FCV and other mobility applications as hydrocarbon upgrader, feed-stock for synthetic fuel and as fuel for hydrogen internal combustion engines (H2ICE) [11]. On the other hand there is the possibility of exploiting hydrogen production from RES in order to create a link between power and gas grids.

Power-to-gas raises as a flexibility measure that could benefit both power and gas grids. It is already possible to blend hydrogen with natural gas and some distribution networks are already familiar with the transportation of mixtures of methane and hydrogen. In general gas grid should tolerate 5% of hydrogen blend at any point of the network and blending up to 10% should not create problem to existing grid [54]. However it is still not sure that every component of the existing grid could operate without problem with blends higher than 1% or 2%. Another possibility for the integration of power and gas grids is the methanation of hydrogen, which despite the additional capital cost and energy losses is able to provide a gas that can be injected in the traditional gas grid without any modification of the existing network. However the methanation process requires high quantities of CO_2, making the whole process reliant on CO_2 capture technologies and their applications, mainly bio-methane production plants. As shown in [5], the injection of hydrogen in the gas grid will not be sustainable in the near or far future, not even in the case of free electricity hydrogen production. The same is inferred by [11], which also propose the methanation of hydrogen as an alternative for the decarbonization of heating and mobility, even if it still suffers from very high costs.

Chapter 3

Methods

This chapter describes the main components of the modeled system as well as the implementation of the model, based on its theoretical basis. All powers and mass flow rates will be referred to a generic time-step.

3.1 System components

The system configuration is described in figure 3.1.

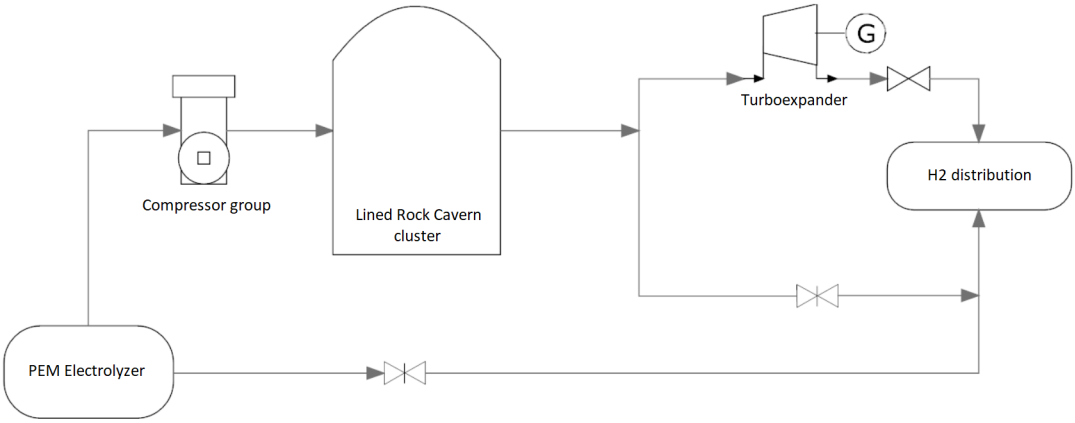

Figure 3.1: System layout

The input flow is given by a PEM electrolyzer which is not included in the model: the flow physical parameters are assumed from literature on PEM electrolyzers [48, 47, 46]. The choice of the technology is based on what already discussed in section 2.5. From the electrolyzer the flow enters the compressor unit and, after being compressed, it is injected in the storage. When required, the high pressure gas is withdrew from the storage and expanded, through a throttle valve or a turboexpander, to a suitable pressure for the injection in the distribution pipeline.

3.1.1 Compressor

The compression unit is based on a reciprocating piston machine, typical of gas compression application, commercially available for a wide range of pressure and flow applications. It is a multi-stage machine with inter-refrigeration to avoid high discharge temperatures at the exit of each stage: this is done in practice to reduce the wear on the equipment and for safety reasons [55]. It is assumed that every refrigeration stage cools down the gas to the injection temperature before entering the next one: in this

way it will be possible to reduce the total number of stages, but at the expenses of larger refrigeration units. Hydrogen compressors guarantee low leakages (in the order of 0.05% of the total mass flow [56]) thanks to reliable sealing applied for safety reasons; moreover high purity hydrogen can be compressed without contamination since the unit is not-lubricated. Besides the model assumes an adiabatic compressor operation.

3.1.2 Hydrogen

Hydrogen is a very low density gas with high mobility compared to other storage gases (natural gas for example). These make the operation of every system, involving hydrogen as working gas, more critical from safety and economic reasons. Hydrogen materials must be chosen wisely in order to avoid corrosion during operation, increasing the cost of each component inside the storage system (compared to natural gas storage). The very low density has an influence on the storage capacity, limiting it when low maximum pressures are considered. Hydrogen behavior can be approximated by ideal gas when very low pressures and ambient temperatures are considered, but it diverts rapidly as pressure increases, as it can be seen from the compressibility factor Z plotted in figure 3.2. In particular $Z = 1$ for ideal gas, so that the more the value of Z is different from 1, the more the gas behavior differs from the ideal gas one. In order to better represent the real behavior of hydrogen, it must be described by means of a real gas equation of state: for this purpose a Matlab tool based on the most recent equation of state has been used [57].

Hydrogen is a liquid below its boiling point of -253°C and a solid below its melting point of -259°C and atmospheric pressure. As shown in figure 3.3, the hydrogen gas phase covers a large span of temperatures and pressures, so that an accurate design of a compressed gas storage plant should not incur in hydrogen or condensation (in particular it can be a concern during the expansion in a turboexpander, hence the necessity to limit the outlet pressure from the machine).

There is a large scientific debate about compressed hydrogen storage, one of the reasons being that in order to compress hydrogen from ambient conditions to very high pressure, it is necessary to spend up to 13% of the the hydrogen energy content [58]. However taking figure 3.4 as reference, it is interesting to notice that the compression power needed at low pressure has a big impact on the whole process, when compressing hydrogen with a multi-stage real machine. That said, if hydro-

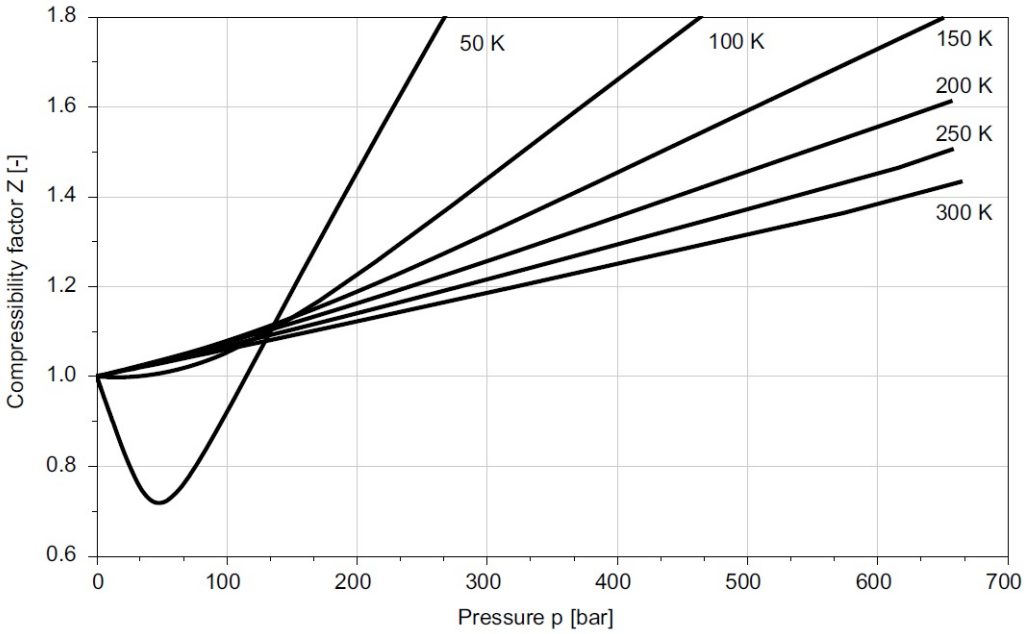

Figure 3.2: Compressibility factor of Hydrogen

gen needs to be compressed starting from a pressure higher than the ambient one, the power required is drastically reduced. This is important to point out when studying electrolyzer-compressor coupling since PEM electrolyzers are able to produce a high pressure gas at their outlet (see section 2.5.1).

Hydrogen poses risks if not properly handled, however the risk must be considered comparable to more common fuels such as gasoline and natural gas. Some hydrogen properties makes it more hazardous, while others can make it less dangerous in different situations. Hydrogen is colorless, odorless and it has a very small molecule, with a great tendency to escape every sealing with high velocity. An eventual leakage of hydrogen is hardly identified by human senses; however it has a lower volumetric energy density, at any pressure, when compared to other gaseous fuels so that every leakage of hydrogen will always contain less energy. Moreover it would disperse much faster since it is more buoyant and diffusive than other fuels. It follows also a lower likelihood of detonation in atmosphere both because it should accumulate reaching a 13%of concentration in air and because it has a flame speed 7 times faster than natural gas or gasoline [60], so that it is most likely to burn instead of detonate.

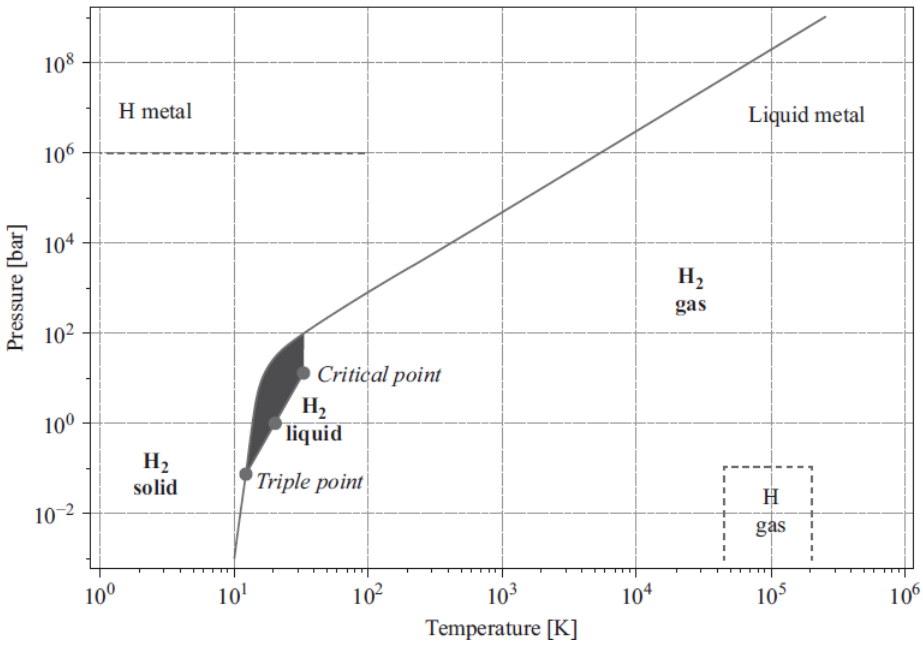

Figure 3.3: Hydrogen phase diagram

3.1.3 Cavern

For the purposes of this study, diverse cavern shapes and properties have been considered. In particular, detailed data shown in table 3.1 have been taken from [44, 61], which are feasibility analysis of hard rock cavern excavation. It is thus possible to suppose the practical possibility to excavate caverns with those defined characteristic. Also they provide detailed costs, used for cost optimization in section 3.2.5.

Since the data refer to a fixed working gas volume of $22,24\text{Mm}^3$ and to a four cavern cluster, they have been characterized in order to obtain the costs for the construction of clusters with a number of caverns from one to four. In this way it is possible to obtain a high modularity for the model simulations. The result of this data-splitting is better described in the cost section 3.2.5.

Regardless the particular configurations, the LRCs considered in the model are supposed to have the same thermo-mechanical characteristics and to be built and treated in the same way, so that it is possible to generalize regarding the structural constraint that must be observed during its operation. The cavern is internally lined with concrete and steel. The reinforced structural concrete lining of 2m thickness is able to smooth the load of the high-pressure gas on the cavern wall, reducing the localized stress on the rock and the possibility of fractures; moreover it provides a more uniform surface for the application of the steel lining. The metal lining only function is to provide an

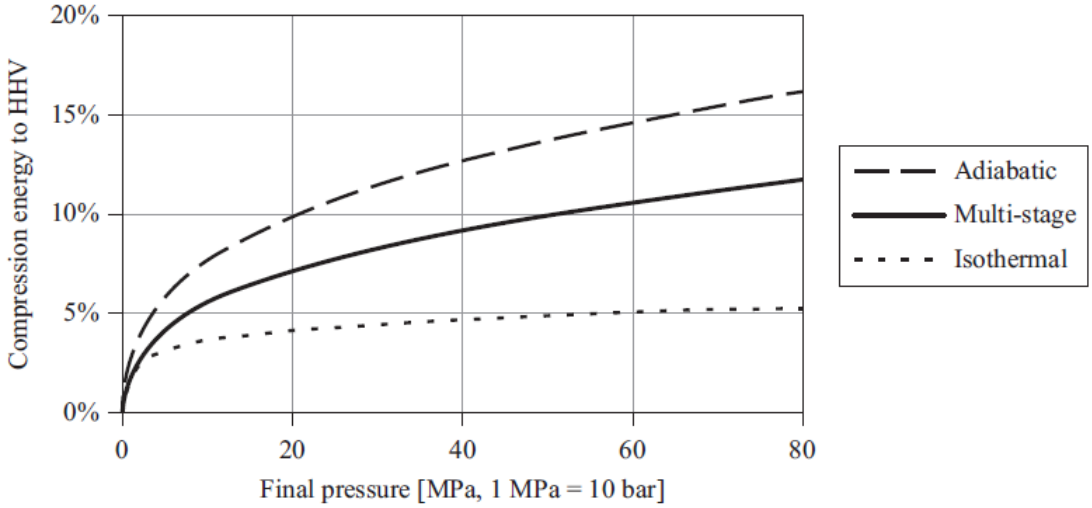

Figure 3.4: Hydrogen compression requirements[59]

impenetrable surface on the cavern wall for the gas; for these reasons the thickness is usually in the order of $13-15$mm. The material used for this application must accommodate moderate deformations due to the cyclic operation of the cavern and be corrosion resistant. Typical austenitic steel based on *Cr-Ni-Mo* are suitable since they do not suffer from atomic interaction with hydrogen. It is possible to evaluate the mass flow of hydrogen through the metal liner with the help of the Fick's Law:

$$J = -D\frac{dC}{dx} \tag{3.1}$$

where D is the *diffusion coefficient*, C the gas *concentration* and J is *diffusion flux* measured in $^{mol}/_{m^2 s}$. It results that for a steel liner with a diffusion coefficient of $0.3 \cdot 10^{-12} {}^{m^2}/_{s}$ for hydrogen, the mass leakage is the order of $3 \cdot 10^{-10} {}^{kg}/_{m^2 s}$ at ambient temperature and 200bar of pressure inside the cavern. This value of leakage would lead to an annual loss of 0.006% of the total cavern mass capacity. With the installation of a metal liner, the only possibilities of gas leakages are by diffusion through the liner itself or through the sealing of the excavation tunnels and injection-extraction wells: here it is assumed that excavation tunnels sealing is perfectly impermeable to hydrogen and that injection and withdrawal processes do not suffer from gas leakages as a direct comparison with oil&gas industry. In conclusion the LRC system is almost completely gas-tight.

As already discussed in section 2.4.2, two parameters that had to be defined a priori are the maximum injection and withdrawal rate, due to the maximum allowable

deformation of the liners and the surrounding rock itself: they were chosen on the basis of the available literature on hydrogen, natural gas and CO_2 underground storage technologies [41, 29, 62]. In the same way it was necessary to define a maximum number of complete charge-discharge cycles (see section 2.4.2), set to 12 based on [41, 63]. Due to the lack of literature on this topic, the main assumption here is that the number of yearly cycles influences the injection and withdrawal rates, setting a maximum yearly flow in and out of the storage. This assumption is only verified if the storage is used to accommodate slow fluctuations throughout the year, showing charge-discharge cycles of about 30 days length. Moreover it is not clear if fast operation at lower pressure (with respect to the maximum one) is beneficial, or not, for the issue of liner fatigue failure: however there are studies on coupled metal/concrete liner capacity to respond to high frequency variation of internal storage pressure [64].

It is also needed to maintain a minimum gas pressure for structural reasons. This lead to the definition of a gas cushion fraction, which is the mass of gas necessary to maintain the minimum defined pressure. From literature on salt caverns (which can be directly applied to hard rock lined cavern for this purpose) its amount ranges from 20% to 30% of the working gas [29, 40]. The definition of the minimum pressure is also important from an economic point of view since the cushion gas volume cannot be recovered and then it represents an investment cost. In order to evaluate the cushion mass it is possible to suppose that, after its injection in the storage, it reaches a stable temperature equal to the surrounding rock, limiting the heat transfer process through the walls. At that moment it is possible to evaluate the gas density as

$$\rho = \rho\left(T, p\right) \tag{3.2}$$

and its mass as $m = \rho V_{st}$ where V_{st} is the total volume of the cavern clusters.

3.1.4 Expander

After the withdrawal from the cavern, the gas pressure must be reduced to match the distribution pipeline pressure. The expansion process can be done with a throttling valve, reducing the pressure without producing power or in a turboexpander, recovering part of the energy spent durin compression. It is clear as the installation of a turboexpander increases both cost and complexity of the plant; on the other hand it could be possible to recover the energy that would be lost with a throttling. The model evaluates both cases and finds the minimum cost configuration.

Hydrogen expanders have already been used for industrial application, so that machines for large scale applications are commercially available. A turboexpander is a centrifugal or axial-flow machine which expands a high pressure gas producing mechanical work, which is after used to drive an electric generator. During the expansion the gas is cooled down depending on the expansion ratio. Hydrogen turboexpanders could reach very low temperature without liquefaction of the gas, due to its low condensation temperature. However considering that hydrogen must be transported in the gaseous phase, limiting technical problems inside the distribution pipelines, in this study the outlet temperature from the expander will be limited to the value defined in section 3.2.3.

3.2 Model implementation

The model describes compression, injection in the cavern and extraction process. Moreover the possibility of installation of an expander for energy recovery purposes has been investigated. The model is based on an 3 hours time-step to simulate the behavior and the cost of the injection and withdrawal processes. Matlab has been used to write the model code.

3.2.1 Injection and withdrawal

Before designing the compression process, it is necessary to evaluate the pressure the compressor must reach through the simulation of the injection/withdrawal processes. Assuming a compressor able to accommodate every necessary pressure variation, it is possible to build a pressure profile that is then given as an input to the compression process simulation, in order to verify the feasibility of the compression process. The mass flow rate coming from the electrolyzer is taken from a simulation of a possible production pattern of a European country, while the demand is supposed to be either constant during the year or a percentage of the electricity consumption (see section 4 for scenarios description). Based on the production flow rates and the maximum injection rate in the cavern, a variable mass flow is injected for each hour of the year. The hydrogen is directly delivered to the distribution pipelines if there is no need to store it or if the system encounters some of the described constraints, as it can be seen in the system scheme in 1. As for the injection, there is a constraint on the withdrawal rate, so that the minimum value between the demand and the maximum rate is actually

withdrew. Both processes must be constrained by the minimum and maximum mass and pressure capacity of the cavern. In particular the minimum mass and pressures are set as already discussed in section 3.1.3, while the maximum values depend on the maximum pressure of the considered cavern. Another constraint on the injection rate is the maximum number of cycle the cavern is able to reach: based on what already discussed in section 3.1.3, the injection rate is reduced by discrete quantities, cycling until the yearly total maximum injection constraint is verified.

Excess of production

Due to the constraints on pressure and in/out flow rates, since the hydrogen production process is not optimized within the developed model, during some hours of the year hydrogen cannot be injected in the storage; in the same way, the withdrawal capacity can limit the hydrogen deliverability. In order to take into account the excess of production or missed delivery, the model considers those as losses in the evaluation of the storage system cost. Since in a real system these conditions are not practical, it has been necessary to find a suitable production pattern among future scenarios of some European countries, through the use of a *GAMS* model developed by the *Energy Division* of *Chalmers University of Technology [65, 66]*, as it will be discussed in section 4. Thanks to this process, it has been possible to limit the cost increase due to hydrogen excess of production or missed delivery, constraining a priori the hydrogen production in order to match the injection and withdrawal limits. The costs found by the model developed in this study have been again implemented inside the GAMS model in order to have a better understanding of hydrogen storage potential in future scenarios.

Heat exchange with the surrounding

During system operation, the temperature inside the cavern fluctuates and gives rise to an heat exchange process between the gas and the surrounding rocks. In order to model the process, some assumptions have been made:

1. rigid container
2. perfect contact between the steel, concrete and rock surfaces
3. the surrounding rocks act as a constant temperature reservoir

The last assumption is based on the high heat capacity of the rock with respect to the one of the cavern. Moreover it is assumed to neglect potential and kinetic energy

in the energy balance equation 3.9: the low H_2 density makes the contribute of the potential energy negligible while, since the injected or extracted mass for each hour of operation is around 1% of the total gas mass inside the cavern, it will only change locally the kinetic energy of the gas, resulting in a negligible overall effect on the stored H_2. Thanks to these assumptions, the heat transfer process can be simplified to a steady state conduction process through two different layers of material and a convective heat exchange between the gas and the internal walls, which can be described by means of a lumped parameters representation as shown in picture 3.5.

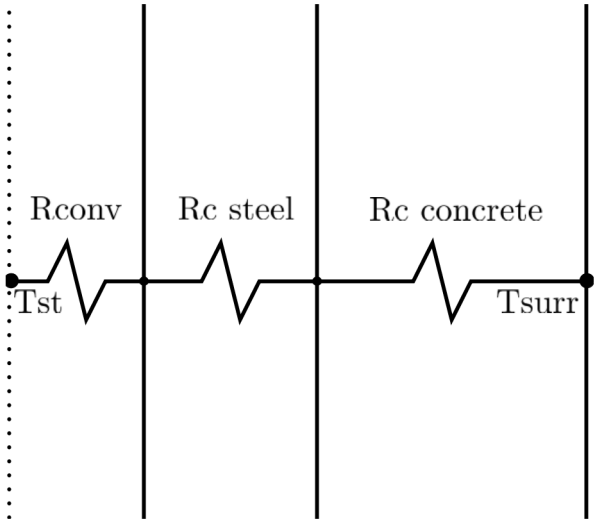

Figure 3.5: Lumped parameter representation

Based on data for steel and structural concrete it is possible to evaluate the resistances: in particular the roof and bottom of the cavern are considered perfectly hemispherical shapes. The conduction resistances through the lateral walls and through the roof and bottom can be written, for a cylindrical geometry, respectively as

$$R_{lat} = \frac{1}{2\pi k_s L} \ln \frac{r_{mean}}{r_{int}} + \frac{1}{2\pi k_c L} \ln \frac{r_{ext}}{r_{mean}} \tag{3.3}$$

$$R_{r-b} = \frac{1}{4\pi k_s} \left(\frac{1}{r_{int}} - \frac{1}{r_{mean}} \right) + \frac{1}{4\pi k_c} \left(\frac{1}{r_{mean}} - \frac{1}{r_{ext}} \right) \tag{3.4}$$

where k is the *thermal conductivity*, L is the height of the cavern cylindrical region and

r_i are the internal, mean and external radii, and the subscripts s and c stand for *steel* and *concrete*, while the lateral convection resistance is evaluated as

$$R_{conv,lat} = \frac{1}{hA_{lat}} \tag{3.5}$$

and the roof and bottom resistances are

$$R_{conv,r-b} = \frac{1}{hA_{r-b}} \tag{3.6}$$

where h is the *convective heat transfer coefficient.* Once the resistances are defined, the heat rate exiting the cavern through the walls can be written as

$$\dot{Q} = \frac{T_{st} - T_{surr}}{R_{lat} + R_{conv,lat}} + 2 \cdot \frac{T_{st} - T_{surr}}{R_{r-b} + R_{conv,r-b}} \tag{3.7}$$

where T_{st} is the mean storage temperature and T_{surr} is the fixed surrounding rock temperature.

Energy and mass balances

To model injection and withdrawal, a system of energy and mass balance must be solved, considering the cavern as a control volume. All the gas properties must be evaluated at the mean gas temperature inside the cavern. Under the assumption of a constant flow rate entering and leaving the system during each time-step it is possible to write the mass balance as

$$\frac{d\rho_{st}}{dt} = \frac{\dot{m}_{in}}{V_{st}} \tag{3.8}$$

and, neglecting potential and kinetic energy as discussed in the heat exchange process description of section 3.2.1, the energy balance for the injection process can be written as

$$\frac{dh_{st}}{dt} = \frac{\dot{m}_{in} h_{in} - \dot{m}_{in} h_{st} - \dot{Q}}{\rho_{st} V_{st}} \tag{3.9}$$

where h_{st} is the *specific enthalpy* of the storage, $\dot{m}_{in}$ in the inlet mass flow rate and V_{st} is the cavern volume. Since the model works with a time step of three hours, balance equations 3.8 and 3.9 can be integrated over the time-step and written as

$$\rho_{st}^{1} = \rho_{st}^{0} + \frac{\dot{m}_{in}^{1}}{V_{st}} \tag{3.10}$$

$$h_{st}^{1} = h_{st}^{0} + \frac{\dot{m}_{in}^{1}\left(h_{in} - h_{st}^{0}\right) - \dot{Q}^{1}}{\rho_{st}^{0} V_{st}} \tag{3.11}$$

where the superscript refers to the time step considered.

Analogously balance equations for withdrawal can be written as

$$\frac{d\rho_{st}}{dt} = \frac{\dot{m}_{out}}{V_{st}} \tag{3.12}$$

$$\frac{dh_{st}}{dt} = \frac{\dot{m}_{out}\, h_{out} - \dot{m}_{out}\, h_{st} - \dot{Q}}{\rho_{st} V_{st}} = -\frac{\dot{Q}}{\rho_{st} V_{st}} \tag{3.13}$$

and integrated on the time step, giving

$$\rho_{st}^{1} = \rho_{st}^{0} + \frac{\dot{m}_{in}^{1}}{V_{st}} \tag{3.14}$$

$$h_{st}^{1} = h_{st}^{0} - \frac{\dot{Q}^{1}}{\rho_{st}^{0} V_{st}} \tag{3.15}$$

3.2.2 Compression

The flow coming from the electrolyzer must be compressed, from the initial pressure to the *injection pressure*, always set at 5bar higher than the cavern pressure. The pressure distribution found in section 3.2.1 is given as input to the compressor. The PEM flow is considered to be at 30bar and 80°C [48, 47, 46]. Before the actual modeling of the compressor it is necessary to define the number of stages of the compressor depending on the maximum pressure needed for the injection: based on the maximum pressure of the considered cavern, the model evaluates the number of necessary stages, simulating a continuous injection in the cavern until its maximum pressure is reached. The number of stages strongly depend on the compressor outlet temperature: if it is assumed to cool down the temperature to the injection temperature of 17°C at each refrigeration stage, the number of stages is fixed to 2 for every cavern configuration; if the compressor is operated to inject a higher temperature gas in the cavern, in order to provide a higher enthalpy content to the expander at the cavern outlet, it varies between 3 and 5 depending on the maximum pressures of the considered cavern. Once the number of

stage is defined it is possible to proceed to the actual compression process. In particular a real compression for a real gas has been considered, defining an isentropic efficiency for the compressor as

$$\eta_{is} = \frac{\Delta h_{is}}{\Delta h_{real}} \tag{3.16}$$

and assuming a value for it of 0.7 based on literature [56, 67, 68]. In particular, the efficiency is strictly dependent on the specific compressor and must be evaluated from case to case. However reciprocating compressor isentropic efficiencies range between $0.60-0.88\%$ and the choice of the value used in the model is driven by the mostly partial operation of the compressor and to avoid under-estimations of the compressor cost and consumption. It is important to recall that the maximum discharge temperature of each stage of the compressor cannot exceed a certain value due to safety and wearing issues: here the need of water inter-refrigeration between the compressor stages. The inter-refrigerated compression process can be described by the following series of equations

$$s_{in} = s_{2,is} = s\left(p_{in}, T_{in}\right) \tag{3.17}$$

$$T_{2,is} = T\left(p_2, s_2\right) \tag{3.18}$$

$$h_{2,is} = h\left(p_2, s_2\right) \tag{3.19}$$

$$h_1 = h\left(p_2, T_{in}\right) \tag{3.20}$$

$$h_2 = \frac{h_{2,is} - h_{in}}{\eta_{is}} + h_{in} \tag{3.21}$$

$$T_2 = T\left(p_2, h_2\right) \tag{3.22}$$

$$s_2 = s\left(T_2, p_2\right) \tag{3.23}$$

where the subscript *in* refers to the inlet of the first compressor stage and the different points are described in figure 3.6. The constraint on the maximum discharge tempera-

ture is always verified at this stage, since this same procedure have been used to evaluate the number of stages for the compressor. In particular the model tries to compress in only one stage, with the constraint on the maximum temperature: if the final temperature is above the fixed value of $135K$, the model increases the number of stages. Finally it is necessary to check that the compression ratio is within an acceptable range. Thanks to this procedure it is possible to map the process for each time-step. The result of the compression process for an intermediate pressure of 123bar is shown in figure 3.6.

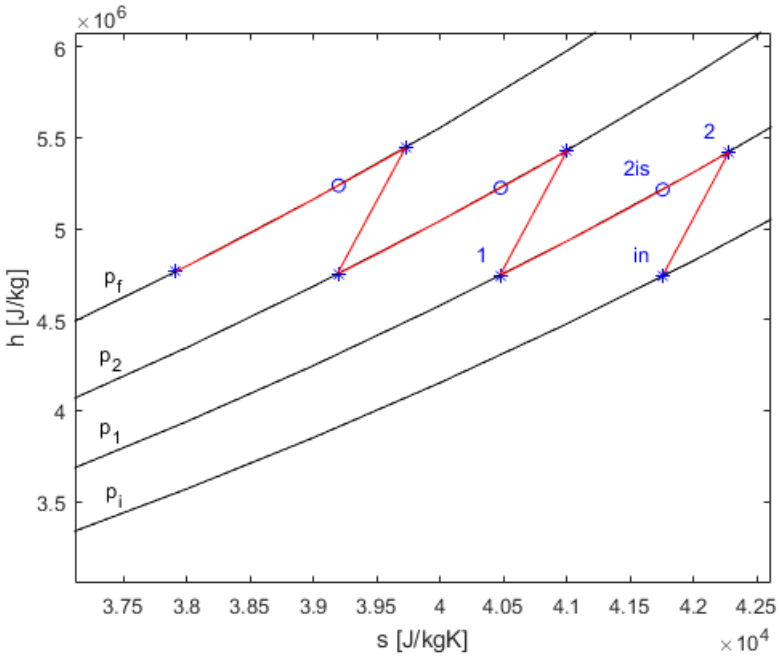

Figure 3.6: Compression process

The last inter-refrigeration process is necessary to bring the gas temperature back to the injection temperature: this is done to avoid a rapid increase of the gas temperature in the cavern, which would lead to a reduction of the overall mass stored and a high heat exchange with the surrounding; moreover a low temperature variation over time is preferable for structural reasons. However when considering the installation of a turboexpander for energy recovery, the last refrigeration stage is no more implemented, meaning that the injection in the cavern happens at the temperature reached by the gas after the last compressor stage. In this way the mean temperature inside the cavern will be higher, allowing one less refrigeration stage and exploiting a higher enthalpy gas in the expander. The refrigeration stages cool down the gas to the injection temperature

before each re-compression, maintaining a higher gas density during the process. For the purpose of simplicity, the process is described by defining an inlet cooling water temperature and an approach point, for gas-liquid heat exchangers, between the exit temperature of the water and the inlet of the gas [69]. Known the gas flow rates with the assumption of adiabatic heat exchangers, it is possible to match the heat exchanged between the two fluids

$$\dot{m}_w \left(h_{w,out} - h_{w,in}\right) = \dot{m}_{gas} \left(h_{g,in} - h_{g,out}\right) \tag{3.24}$$

where every specific enthalpy is evaluated as $h = h\left(T, p\right)$.

Consequently the necessary water flow rate is

$$\dot{m}_w = \frac{\dot{m}_{gas} \left(h_{g,in} - h_{g,out}\right)}{\left(h_{w,out} - h_{w,in}\right)} \tag{3.25}$$

This relation can be applied to every inter-refrigerator in order to evaluate the diverse necessary water flow rates.

3.2.3 Expansion

An expander could be required in a hydrogen storage plant in order to recover part of the energy spent for the compression process. The expander is located directly at the outlet of the cavern so that it will operate discontinuously, based on the hydrogen demand required. The expansion ratio will not be fixed, since it is necessary to avoid too low temperature at the outlet of the expander; moreover it will depend on the the gas conditions at the cavern outlet (temperature and pressure). It is then possible to model the expansion similarly to the compression process: assuming an *isentropic expansion efficiency* $\eta_{is,exp}$, a minimum temperature and pressure at the exit of the expander (10°C, 20bar [70]) and considering the real gas properties it is possible to write

$$h_{st} = h\left(p_{st}, T_{st}\right) \tag{3.26}$$

$$s_{st} = \left(p_{st}, T_{st}\right) \tag{3.27}$$

$$h_{f,is} = h\left(s_{st}, p_f\right) \tag{3.28}$$

$$h_f = h_{st} - \eta_{is,exp} \left(h_{st} - h_{f,is}\right) \tag{3.29}$$

$$T_f = T\left(h_f, p_f\right) \tag{3.30}$$

where the subscript *st* refers to the storage gas conditions, f refers to the conditions after the expansion, $\eta_{is} = 0.8$ is taken from [71, 72] and considered to be lower due to discontinuous and unrated operation. The process described above is then cycled until a suitable temperature after the expander is reached, increasing the final pressure at each step. The result is a different final pressure for each time-step and, as a result, variable enthalpy steps $\Delta h = h_{st} - h_f$ inside the expander. The expander outlet gas will be then throttled to the final pipeline pressure. The electric power produced by the expander for each time-step is

$$P_{exp} = \Delta h \dot{m}_{out} \eta_{elm} \tag{3.31}$$

with electro-mechanical efficiency $\eta_{elm} = 0.95$. Finally it is possible to define a *recovery efficiency* as

$$\eta_{rec} = \frac{E_{exp}}{E_{comp}} \tag{3.32}$$

which represents the percentage of electric energy consumed by the compressor that can be recovered with the installation of a hydrogen turboexpander, where the electric energy produced by the expander in one year of operation is $E_{exp} = \sum_{year} P_{exp}$ and analogously $E_{comp} = \sum_{year} P_{comp}$ for the compressor.

3.2.4 Efficiency

Before proceeding to the definition and evaluation of a system efficiency, it is necessary to evaluate the power consumption of the system components.

Starting with the compressor, the power consumption for each time-step is evaluated as

$$P_{comp} = \frac{1}{\eta_{m-el}} \dot{m}_{gas} \sum_{1}^{n_{stages}} \Delta h_{stage,i} \tag{3.33}$$

where the *mechanical-electrical efficiency* η_{m-el} is taken from reciprocating compressor literature [67]. Water pumps consumption is evaluated choosing a reasonable pressure loss inside the refrigerators, even if this piece of information is hard to be found without a proper heat exchanger design (however as it can be seen in the section 4, the power consumption of the pumps is always around three order of magnitude lower

than the compressor one, even over a wide range of pressure drops, making the choice of a realistic pressure loss not significant)

$$P_{pump} = \frac{\dot{m}_w \Delta p}{\eta_m \eta_{el} \rho_w} \tag{3.34}$$

where $\dot{m}_w$ is the total water mass flow rate and η_m and η_{el} respectively the mechanical and electrical efficiencies.

In order to find an efficiency for the overall process, it is common practice to use the LHV energy of H_2 as the inlet energy in the system [60, 30]: it is then possible to evaluate the energy losses due to compression and mass leakages with respect to a common reference energy. The yearly system efficiency can be written as

$$\eta_{sy} = \frac{m_{gas}\,(1-\eta_{leak})\,LHV_{H_2} - E_{comp} - E_{pump}}{m_{gas} LHV_{H_2}} \tag{3.35}$$

where $\eta_{leak} = 0.5\%$ expresses the losses due to *mass leakages* during the compression stage. Moreover it is also possible to evaluate an hour-by-hour efficiency, considering mass flows and power instead of masses and energies, as

$$\eta_{sy,i} = \frac{\dot{m}_{gas,i}\,(1-\eta_{leak})\,LHV_{H_2} - P_{comp,i} - P_{pump,i}}{\dot{m}_{gas,i} LHV_{H_2}} \tag{3.36}$$

which will represent the system efficiency for each time-step. However it is not representative of the final performance of the system. The yearly efficiency value will instead represent how well the system performs in extracting most of the entering chemical energy, during a year of operation. Thus in order to evaluate η_{sy} it is necessary to simulate the system operation and its value will again depend on the maximum pressure of the considered cavern (see section 4.1). It is also necessary to specify that, in the case of installation of an expander for energy recovery, the system efficiency definition will slightly differ

$$\eta_{sy} = \frac{m_{gas}\,(1-\eta_{leak})\,LHV_{H_2} - E_{comp} - E_{pump} + E_{exp}}{m_{gas} LHV_{H_2}} \tag{3.37}$$

taking into account the energy recovery component E_{exp}.

3.2.5 Costs

The cost estimation process is based on the three main components of the system: compressor, expander and cavern.

Compressor and expander

As already discussed in section 3.1.1, reciprocating compressors for hydrogen applications are commercially available. The cost estimation is thus based on the tool *"H2A Delivery Components Model"* developed by the *USA Department of Energy* [56], which relies directly on compressor producers costs. The compression section of the model produces the inputs for the tool, which in turn is able to return investment and O&M costs, again implemented in the final cost evaluation in the Matlab model. Moreover it was necessary to compare sizing and consumption of the compressor units given by the tool with the results of the Matlab model, in order to check the consistency of the cost evaluation. The compressor section of the system is composed by three units (oversized by10%), one of them in stand-by: this design choice was necessary to achieve a higher availability during compression. Moreover they have been designed based on the number of stages and the isentropic efficiency, as already discussed in section 3.2.2. The results of the tool depend on the compressor sizing, which in turn depends on the hydrogen production flow rates and cavern dimension, since it will limit the injection capacity and so the gas flow that must be compressed.

Investment cost for the turboexpander are taken from [72], while the O&M yearly costs are supposed to amount to the same percentage of the total investment as for the compressor. An accurate estimation of these costs is not possible since they vary for every application. However, in order to avoid an underestimation of the costs, the investment cost has been supposed to be $1500\,\$/\mathrm{kW}$ where the very broad range found in literature was $600 - 2300\,\$/\mathrm{kW}$.

Cavern

Cost data about cavern excavation and related facilities construction have been taken from [44], since their detailed classification fits well the purposes of this study. As already discussed in section 3.1.3, they have been adapted to be used as input for the model. In table 3.2 it is possible to see how they have been specified with respect to the initial form shown in table 3.1, and how every characteristic of the cavern influences its cost; however this topic will not be discussed, since a geomechanical analysis has already been shown in [44].

In particular the main difference in cost, between clusters integrating a different number of cavern, is related to the excavation of the access tunnel, since more than one cavern can be accessed by the same tunnel. This means that clusters with a higher

number of caverns will have a lower cost of excavation per single cavern, once fixed the working gas volume. O&M cost are not specified for the cavern, since it is supposed that they are already included in the compressor O&M variable and fixed yearly costs.

Net Present Cost

On the basis of the cost evaluated in sections 3.2.5 and 3.2.5 it is possible to define and evaluate the *Net Present Cost* as

$$NPC = \sum_{k=1}^{N} \frac{C_{ep} + C_{md} + O\&M}{(1+r)^k} + C_0 \tag{3.38}$$

where r is the *real discount rate* defined as

$$i = \frac{1+d}{1+i} - 1$$

being $d = 0.1$ the *normal discount rate* and $i = 0.02$ the *inflation rate*; $N = 25$ is the system lifetime, $C_0 = C_{comp} + C_{cav} + C_{exp}$ the total investment cost comprehensive of the compressor, turboexpander and the cavern costs; in particular the latter is divided in the actual cavern cost (defined in table3.2) and the cushion gas cost

$$C_{cushion} = m_{cushion} c_{prod\,H_2}$$

where $c_{prod\,H_2} = 5.12 \$/\text{kg}$ [73] is the production cost of hydrogen from a PEM electrolyzer; C_{ep}= *cost of excess of production* and C_{md}=*cost of missed delivery* are defined as follows

$$C_{ep} = c_{prod\,H_2} m_{ex-prod} \tag{3.39}$$

$$C_{md} = p_{H_2} m_{miss-del} \tag{3.40}$$

where $p_{H_2} = 5 \$/\text{kg}$ [20] is the hydrogen retailing price, $m_{ex-prod}$ and $m_{miss-del}$ represent respectively the excess mass of hydrogen produced and the mass not delivered to the distribution pipelines; $O\&M$ cost are specified both for the compressor and the expander. The NPC is used by the model in order to identify the most cost efficient cavern in a 25 years life-time of the system. In order to compare different cavern configurations or costs in different hydrogen production scenarios, it is better to define the *specific cost of storage* $c_{storage}$ and the *specific cost of delivery* $c_{delivery}$ of hydrogen from the storage

$$c_{storage} = \frac{NPC/N}{E_{wg}} \tag{3.41}$$

$$c_{delivery} = \frac{NPC/N}{LHV_{H_2} m_{inj}} \tag{3.42}$$

where E_{wg} is the working gas energy and $m_{inj} = \sum_i m_{inj,i}$ is the yearly mass of hydrogen injected in the storage, which express respectively the specific cost of the system to store 1kWh of hydrogen in the hypothesis of no cyclability of the cavern and the specific cost of the system to delivery 1kWh of hydrogen when the cavern is cycled within its maximum capacity. In the same way it is possible to evaluate the *specific cost per* kg *of delivery* and the *specific cost per* kg *of storage* as

$$c_{storage,kg} = \frac{NPC/N}{m_{wg}} \tag{3.43}$$

$$c_{delivery,kg} = \frac{NPC/N}{m_{inj}} \tag{3.44}$$

where m_{wg} is the working gas mass. Results given by equations 3.41 and 3.42 refer to the LHV content of the gas, while it is possible to refer the costs to the electricity delivery by the definition of a *power unit efficiency*, defined as the hydrogen energy spent to produce electricity

$$\eta_{pu} = \frac{E_{el}}{LHV_{H_2}}$$

This value will depend on the specific power unit, as it is possible to use hydrogen to produce electricity both in gas turbines and in hydrogen fuel cells, where it is possible to further distinguish between the different available technologies. In particular it is important to specify a main assumption of the following calculations: it is assumed that the power unit for hydrogen conversion is not included in the cost evaluation, assuming that an already existing plant could be used to produce electricity without capital investment or increased maintenance. In this way it is possible to express costs in $[\$/\mathrm{kWh_{el}}]$ by dividing equations 3.41 and 3.42 by the power unit efficiency η_{pu}

$$c_{storage,el} = c^*_{storage}/\eta_{pu} \tag{3.45}$$

$$c_{delivery,el} = c^*_{delivery}/\eta_{pu} \tag{3.46}$$

where an arbitrary value of $\eta_{pu} = 0.60$ has been used based on a benchmarking of the actual efficiencies of combined cycle power plants [11, 74] and $c^*_{storage}$,$c^*_{delivery}$ are the modified specific costs evaluated considering an additional electrolysis cost component in the NPC cost equation 3.38, which has been fixed at $5.12\$/\text{kg}$, based on an electricity cost of $6.22\$/\text{kWh}$ and an electrolyzer electrical consumption of $50.2\text{kWh}/\text{kg}$ [73]. In particular this is done in order to be consistent and express a final electricity production cost as the result of a full AC-AC conversion; moreover it will be possible, in this way, to compare the studied system with other electricity storage technologies.

It is also interesting to analyze costs in relation to the mobility sector, since it seems to be the most promising in terms of development of hydrogen economy (see section 2.6). In particular, starting from the modified delivery cost of hydrogen $c^*_{delivery}$, it is possible to find the final cost of mechanical power delivery (or operation cost) considering a *tank to wheel* efficiency η_{TTW}, defined as the mechanical energy produced by the vehicle over the entering chemical energy of hydrogen, from equation

$$C_{FCEV} = c^*_{delivery}\eta_{TTW,FCEL} \tag{3.47}$$

which is expressed in $[\$/\text{kWh}_\text{m}]$. The same procedure can be done with battery electric vehicles (BEV)

$$C_{BEV} = c_{electricity}\eta_{TTW,BEV} \tag{3.48}$$

with the main difference that in this case the entering energy is in the form of electricity; it is then possible to make a comparison between the two final costs.

P[bar]	Depth[m]	Diameter[m]	Vol[m^3]	Height[m]	Cost[$/$m^3$]
100	150	15	1,78E+05	241,38	5,92
150	150	15	1,22E+05	162,62	4,5
200	150	15	9,43E+04	123,48	3,8
100	200	15	1,78E+05	241,38	5,95
150	200	15	1,22E+05	162,62	4,54
200	200	15	9,43E+04	123,48	3,83
100	250	15	1,78E+05	241,38	5,99
150	250	15	1,22E+05	162,62	4,57
200	250	15	9,43E+04	123,48	3,87
100	150	20	1,78E+05	128,07	5,05
150	150	20	1,22E+05	83,77	3,94
200	150	20	9,43E+04	61,75	3,39
100	200	20	1,78E+05	128,07	5,08
150	200	20	1,22E+05	83,77	3,97
200	200	20	9,43E+04	61,75	3,42
100	250	20	1,78E+05	128,07	5,12
150	250	20	1,22E+05	83,77	4,01
200	250	20	9,43E+04	61,75	3,46
100	150	25	1,78E+05	73,83	4,6
150	150	25	1,22E+05	45,48	3,67
200	150	25	9,43E+04	31,39	3,2
100	200	25	1,78E+05	73,83	4,63
150	200	25	1,22E+05	45,48	3,7
200	200	25	9,43E+04	31,39	3,24
100	250	25	1,78E+05	73,83	4,67
150	250	25	1,22E+05	45,48	3,74
200	250	25	9,43E+04	31,39	3,27
100	150	30	1,78E+05	42,85	4,36
150	150	30	1,22E+05	23,16	3,54
200	150	30	9,43E+04	13,37	3,14
100	200	30	1,78E+05	42,85	4,39
150	200	30	1,22E+05	23,16	3,58
200	200	30	9,43E+04	13,37	3,17
100	250	30	1,78E+05	42,85	4,43
150	250	30	1,22E+05	23,16	3,61
200	250	30	9,43E+04	13,37	3,21

Table 3.1: Cavern data

					Investment cost [M$]			
#conf	P[bar]	Depth[m]	D[m]	H[m]	4 cav	1 cav	2 cav	3 cav
1	100	150	15	241,38	132	38	69	100
2	150	150	15	162,62	100	30	53	77
3	200	150	15	123,48	85	26	45	65
4	100	200	15	241,38	132	38	69	101
5	150	200	15	162,62	101	30	54	77
6	200	200	15	123,48	85	26	46	65
7	100	250	15	241,38	133	38	70	101
8	150	250	15	162,62	102	30	54	78
9	200	250	15	123,48	86	26	46	66
10	100	150	20	128,07	112	33	59	86
11	150	150	20	83,77	88	27	47	67
12	200	150	20	61,75	75	24	41	58
13	100	200	20	128,07	113	33	60	86
14	150	200	20	83,77	88	27	47	68
15	200	200	20	61,75	76	24	41	59
16	100	250	20	128,07	114	33	60	87
17	150	250	20	83,77	89	27	48	68
18	200	250	20	61,75	77	24	42	59
19	100	150	25	73,83	102	30	54	78
20	150	150	25	45,48	82	25	44	63
21	200	150	25	31,39	71	22	39	55
22	100	200	25	73,83	103	30	55	79
23	150	200	25	45,48	82	25	44	63
24	200	200	25	31,39	72	23	39	56
25	100	250	25	73,83	104	31	55	79
26	150	250	25	45,48	83	26	45	64
27	200	250	25	31,39	73	23	39	56
28	100	150	30	42,85	97	29	52	74
29	150	150	30	23,16	79	24	43	61
30	200	150	30	13,37	70	22	38	54
31	100	200	30	42,85	98	29	52	75
32	150	200	30	23,16	80	25	43	61
33	200	200	30	13,37	71	22	38	54
34	100	250	30	42,85	99	29	52	75
35	150	250	30	23,16	80	25	43	62
36	200	250	30	13,37	71	23	39	55

Table 3.2: Cavern costs characterized by cluster dimension

Chapter 4

Results

The most relevant results of the study will be presented in the following. Four different hydrogen production scenarios have been considered, running the simulation for the case with no expander for recovery, referred as the "base case" and the case with the installation of a turboexpander at the cavern outlet, referred as the "expander case", for a total of 8 simulations. The hydrogen production data have been chosen to be representative of four different caverns operation and dimension: in particular, with the help of a GAMS electricity grid model developed by the Energy Division of the Earth, Space and Environment department of Chalmers University of Technology, it was possible to obtain diverse hydrogen production patterns, considering eventual raw hydrogen demand, system costs and power production mix constraints. The considered scenarios, however, have to be considered as test inputs, useful to validate the model and draw final consideration about the storage plant operation. The main assumptions of the GAMS model, used to obtain the input data, are described in section 4.3. Scenarios SC3 and SC4 are better described in section 4.3, respectively referred as "*expensive both, H_2 demand*" and "*original, noBio*"; scenarios SC1 and SC2 are both referred as "*original, noBio*" but have been obtained with different assumed initial values for the hydrogen storage plant cost. In particular very high costs (with respect to what are the results of this study) were assumed for those two scenarios, respectively 11€/kWh and 44€/kWh and based on what found in [75], which were mostly useful to obtain completely different storage utilization patterns and better prove the model functioning. Moreover higher assumed costs have result in higher cost results, proving convergence between costs in the case of an eventual optimization process involving the two models.

For each scenario the model evaluates the cavern configuration with the lower NPC among the ones described in table 3.2. Only the most cost effective cavern among all the configuration will be described for each scenario and case. Table 4.1 shows the chosen cavern configuration as well as the cluster configuration (see section 3.1.3, #x=number of clusters of x caverns), the mass capacity and the energy capacity (referred to the hydrogen LHV) for each case and scenario.

4.1 Thermodynamic analysis

The system operation is described through the variation of the thermodynamic state of the gas inside the storage and the energy consumption and production of the external components (compressors, pumps and expander). For every H_2 production scenario

	#conf	#4	#3	#2	#1	Mass [t]	Energy [GWh]	η_{sy}
$SC1, base$	30	7	1	0	0	7855	262	0.9728
$SC1, expander$	30	7	1	0	0	7855	262	0.9719
$SC2, base$	28	1	1	0	0	1172	39	0.9810
$SC2, expander$	31	1	1	0	0	1172	39	0.9798
$SC3, base$	29	1	0	0	0	1014	34	0.9726
$SC3, expander$	30	1	0	0	1	1123	37	0.9763
$SC4, base$	30	24	1	0	0	25086	836	0.9751
$SC4, expander$	30	24	1	0	0	25086	836	0.9737

Table 4.1: NPC optimization results

the system will behave differently, as it will produce different results in the expander case with respect to the base case, making possible a comparison from two different points of view.

4.1.1 Scenarios comparison

The cavern operation can be well described through the use of a pressure/density against time-steps diagram, which will express how and when the gas is injected or withdrew from the cavern. In figure 4.1 it is possible to see how pressure and density inside the cavern follow the same trend in every scenario (the same behavior is found in the expander cases). This is reasonable since the narrow temperature variation in the cavern, which is due to the fixed injection temperature, similar to the surrounding rock one in order to limit the heat exchange process and shown in figure 4.2 for $SC1, base$ (similar behavior is found in every base case scenario).

It is possible to explain the density behavior when considering the $T-s$ equilibrium diagram of hydrogen behaving as a real gas, since the density variation is much more influenced by a pressure variation with respect to a temperature variation, as it can be seen from figure 4.3, pointing out how the density curves are only slightly steeper than the pressure curves.

Different scenarios will provide different cavern dimension as well as injection and withdrawal rates, since they are directly proportional to the cavern volume: in the $p-t$ diagram shown in figure 4.1 it is possible to see how increases and decreases of pressure are steeper for the scenarios with larger cavern capacity. Moreover the pressure is always constrained between the minimum and maximum values defined in the cavern design phase. Pressure, temperature and density variations are the results

of the injection, withdrawal and heat exchange processes which happen independently one from each other.

The recovery efficiency defined in eq.3.32 will depend on the cavern operation, in particular on the temperature and pressure conditions of the cavern outlet gas. Higher mean operating pressure and temperature will allow a higher energy recovery in the turboexpander, providing larger enthalpy drops inside the machine before reaching the minimum outlet temperature, as discussed in section 3.2.3. Values of the recovery efficiency are found in table 4.2.

η_{rec}	$SC1$	$SC2$	$SC3$	$SC4$
%	9	10	10	7

Table 4.2: Recovery efficiency in the expander case

Due to the low values found for the recovery efficiency, the installation of the turboexpander seems to be not conveniente in the considered scenarios (see sections 4.1.24.2).

System efficiencies for every scenario are shown in table 4.1, based on the definition given in equations 3.35 and 3.37; they show high values, oscillating between $97-98\%$: it is reasonable to have low losses with the design choices of this study. In particular mass losses are only supposed to happen in the compressing unit (they account for 0.5% of the total mass flow rate); the compressor power consumption is limited since the gas must be compressed from an already high starting pressure of 30bar (outlet pressure of the electrolyzer unit) to a relatively low maximum pressure of $100-200$bar (see section 3.1.2) and pumping losses are almost negligible, being 2 orders of magnitude lower than the electricity spent for compression. In figure 4.4 it is possible to see how the efficiency is influenced by the starting pressure, where the results are obtained from the simulation of a continuous filling of one cavern with a maximum pressure of 200bar (configuration 30, table 3.2). It is thus interesting to notice how, compressing the gas from a pressure of 30bar, it is possible to save up to 7% of the gas LHV content during compression, since the energy losses are already accounted in the PEM electrolyzer efficiency.

Moreover figure 4.5 shows the efficiency variation with respect to the final pressure, compressing from 30bar and in the same cavern configuration of figure 4.4. It is clear how the energy consumption of the compressor is slowly increasing when approaching high pressures, thus it possible to infer that higher maximum pressure caverns will always show a lower overall efficiency.

4.1.2 Cases comparison

The first operating parameter strongly influenced by the different operating conditions between the base case and the expander case is the gas temperature inside the cavern. Figure 4.6 show the temperature behavior during an year of operation for the expander case in every scenario. It is possible to compare it with figure 4.2 to notice how the mean cavern temperature remains always higher during operation.

This temperature behavior leads to a reduced overall capacity of the cavern due to a decrease of the gas density, as it will be discussed in the following. However the operative choice of injecting the gas in the cavern at high temperatures leads to an overall increased enthalpy content of the gas, which can be exploited in the turboexpander for recovery.

Due to the constraints on the minimum and maximum pressure of the cavern, the model will limit injection or withdrawal when the cavern pressure is close to those values. In particular all the scenarios do not exceed the injection limit, but this happens for the withdrawal limit. This means that for every scenario there will be a partial missed delivery (see section 3.2.5, eq.3.40), expressed as a percentage of the total demand and shown in table 4.3.

	SC1,b	SC1,e	SC2,b	SC2,e	SC3,b	SC3,e	SC4,b	SC4,e
Missed del[%]	4,3	4,7	5,1	4,7	4,7	3,2	9,9	9,8

Table 4.3: Missed delivery

In particular the withdrawal process is limited in two different operating conditions: when the cavern pressure is close or equal to the minimum value or when the maximum withdrawal constraint is reached. It is possible to notice how in the expander case, for 3 out of 4 scenarios, the missed delivery has a lower value despite the lower maximum capacity of the cavern. The higher mean temperature in the cavern decreases indeed the mean gas density, decreasing the maximum mass that can be injected: a mean temperature range of $25-30°C$ causes a reduction of the maximum capacity of $4-5\%$ along all the different cavern configuration and maximum pressures, with respect to a mean temperature of 17°C, as set in the base case. However, when operating in the lower range of pressures, the system can benefit of a lower density, boosting up the pressure and allowing withdrawals, as it is clear from figure 4.8 between the 1000^{th} and 1500^{th} time step, where the pressure in the expander case is significantly higher than in the base case (even if the diagram is referred to the gas energy content, its density

is strongly influenced by pressure as discussed in 4.1.1, so that pressure, density and LHV content will follow almost the same trend). Figure 4.7 shows a scatter plot of the missed delivery against time-steps and compared to the cavern pressure for *SC*3 in both study cases, allowing to locate in time the single missed deliveries.

In particular the withdrawal process cannot happen if the pressure is close to the minimum one, loosing all the demand for that time-step, while it is only reduced of a certain quantity, related to the excess of demand, when the withdrawal limit is reached. Even if the maximum cavern capacity is reduced, this does not mean that the maximum exploited capacity is also reduced: as it can be seen from figure 4.8, the maximum energy reached by the cavern is higher in the expander case for *SC*2 (with same maximum pressure cavern for both cases), allowing to infer that every scenario and subsequent plant design will differ from case to case.

Nonetheless, in general, the maximum capacity is lowered, causing reduced injection capabilities in the cavern which in turn is reflected in a lower cyclability of the storage system. This could have a huge impact on the cavern operation and final cost, as it will be discussed in section 4.2 (see section 3.1.3).

4.2 Costs analysis

The cost analysis is based on the main components of the system: compressors, caverns and expander; cost have been evaluated on the basis of what discussed in section 3.2.5.

In table 4.4 the most relevant cost optimization results are reported, based on eq. 3.41, 3.42, 3.43, 3.44, reporting the maximum cavern energy capacity and number of yearly cycles for comparison.

	$c_{storage}$ [$/kWh]	$c_{delivery}$ [$/kWh]	$c_{delivery,kg}$ [$/kg]	$c_{storage}$ [$/kg]	$Energy$ [GWh]	cycles
$SC1, base$	2,30	0,009	0,29	77	262	10,7
$SC1, expander$	2,49	0,009	0,31	83	262	10,7
$SC2, base$	3,57	0,014	0,48	119	39	9,8
$SC2, expander$	3,74	0,015	0,51	125	39	9,8
$SC3, base$	2,66	0,010	0,33	89	34	10,8
$SC3, expander$	2,64	0,011	0,36	88	37	9,7
$SC4, base$	2,28	0,015	0,50	76	836	6,0
$SC4, expander$	2,30	0,015	0,51	77	836	6,0

Table 4.4: Cost results

Looking at the results it is possible to firstly notice that there are not system econ-

omy of scale, since higher storage capacities does not lead to lower specific costs. However this study is already focusing on large scale applications and the cost estimation is already considering economies of scale on the single components. Moreover, as it can be seen in figure 4.9, the largest portion of investment is occupied by the cavern, which in this study does not respond to scale enlargement linearly: once a cluster of 4 caverns has been selected, the 5^{th} cavern will cost more than the 4^{th} as well as the 9^{th} will cost more than the 8^{th} and so on.

As introduced in section 4.1.2, the cyclability of the storage has a clear result on its cost. From 4.4 it is clear how an higher number of yearly cycles leads to a lower specific cost of delivery. In particular the lowest cost of delivery is produced in $SC1$ where the cavern is cycled $10,7$ times per year, while the higher costs are found in $SC2$ and $SC4$. However $SC2$ shows considerably higher investment costs, so that the higher number of cycles, with respect to $SC4$, does not compensate for the final delivery cost. $SC3,base$ shows higher investment costs with respect to $SC1,base$ which is reflected in slightly higher delivery costs, being the number of yearly cycles similar. Thus the importance of exploiting the cavern cyclability to reduce overall delivery cost of hydrogen. It is interesting to compare these results with the costs found in literature (see section 1.1, figure 1.4): the specific cost of storage for rock caverns found in literature finds its maximum value in $50^{\$}/_{kg}$, while this study has shown a cost range of $76-125^{\$}/_{kg}$. This discrepancy could be partially attributed to the absence of an internal liner and partially to the lack of extensive information about underground rock caverns storage. However when considering the delivery cost, it seems to be aligned to the literature values in the most expensive scenarios, while significantly lower in the two cheapest scenarios $SC1$, $SC3$. Further research on the cyclability capacity of LRC storage could help increasing the cost knowledge of this particular technology.

Figure 4.10 shows the yearly expenses for the storage facility for every case and scenario. It is clear how the most important contribution, after the cavern investment, is due to $O\&M$ costs of the compression units. Those costs are dominated by the cost of electricity consumption to drive the compressor, which amounts to $75-77\%$ of the total compressor cost: in a system optimization logic these costs could be reduced, optimizing hydrogen production together to its compression to better exploit the market electricity price arbitrage. With reference to table 3.2, it can be noticed that the 30^{th} cavern configuration is the cheapest one in terms of capital investment. However, even if most of the scenarios have their cost optimized in that configuration, some of them do not. In particular in $SC2$ the optimal configuration is a bigger cavern with lower

maximum pressure (100bar), meaning that this particular scenario could benefit of a reduced compression cost both in terms of investment (compressor size) and electricity consumption. The different choice in terms of cavern configuration between $SC2, base$ and $SC2, exp$ can be justified saying that the latter can take advantage of a slightly higher surrounding rock temperature, since it is located 50mdeeper underground.

Starting from eq. 3.46 it is also possible to show the systems cost to delivery electricity and compare it with other technologies. Please refer to figure 4.11.

Based on the actual cost of hydrogen produced from PEM electrolyzers of $5.12\,\$/\mathrm{kg}$ [73], the delivery cost of electricity $c_{delivery,el}$ from a hydrogen storage plant results in the range of $0.26 - 0.27\,\$/\mathrm{kWh_{el}}$. This value is consistent with what found in literature on hydrogen application (see figure 1.3). However PEM hydrogen production cost is based on an electricity price of $6.22\,\mathrm{c\$}/\mathrm{kWh}$ and an electrolysis electrical consumption of $50.2\,\mathrm{kWh}/\mathrm{kg}$, meaning that electricity cost is responsible of more than 60% of the total cost. A cost analysis of electricity delivery, considering a PEM electrolysis cost of $2\,\$/\mathrm{kg}$ (ideal scenario in which hydrogen can be produced from free electricity, for example avoiding curtailment), would lead to $c_{delivery,el} = 0.11 - 0.12\,\$/\mathrm{kWh_{el}}$. Moreover, when considering the future trend in the PEM electrolyzers costs, it is found that it will be possible to produce hydrogen for large-scale central applications for $4.2\,\$/\mathrm{kg}$ already in 2025 [73], leading to $c_{delivery,el} = 0.22 - 0.23\,\$/\mathrm{kWh_{el}}$ or in the ideal scenario of free available electricity $c_{delivery,el} = 0.05 - 0.07\,\$/\mathrm{kWh_{el}}$. The results are consistent with literature findings, shown again in figure 4.12: hydrogen is actually economically competitive with most of the battery applications, but it is not with PHS and CAES if the actual full price of electricity is considered. Only the possibility of exploiting very low electricity prices during off peak demand could lead to sustainable, grid connected, hydrogen storage systems.

However delivery costs of hydrogen from LRC systems only remain low, having a marginal impact on the overall system investment: grid-connected hydrogen storage systems will mostly depend on future improvement of electrolysis costs and performances.

On the other hand, the creation of a differentiated hydrogen market could increase the interest of a direct use of hydrogen, as discussed in section 2.6. Since mobility will probably be the main driver of the future hydrogen economy, it is relevant to make some short considerations about the cost of FCEV in comparison with the competitors. In particular, looking at a future dominated by CO_2 regulation and with increased attention to emission control, it was chosen to consider BEV as frame of reference.

Based on equations 3.47 and 3.48 it is possible to compare BEV and FCEV in terms of cost performances. Values of η_{TTW} of 0.83% and 0.48% have been used respectively for BEV and FCEV [77], which gives costs results of respectively $0.08^{\$}/_{kWh_m}$ and $0.07 - 0.30^{\$}/_{kWh_m}$, where the latter is the value referred to the delivery cost of hydrogen in 2025 and ranges between an electricity cost of $0 - 6.89^{\$}/_{kWh}$. These are only the costs to run the vehicle and do not take into account the production cost of it: in particular FCEV costs are now lower than BEV and are supposed to be further reduced in the near future, remaining always below BEV trends and eventually reaching the same value after 2040 [78, 79] . It is not possible to state which technology will be more convenient in a future mobility scenario, since the above considerations only consider the production cost of vehicles and the cost of production and storage of H_2, excluding from the equation all the cost related to the hydrogen distribution and retail infrastructure development, which will raise as the big challenge of the future hydrogen economy.

4.3 Hydrogen cost impact on future scenarios

There is uncertainty on the actual and future costs of every component of a hydrogen production and storage system. Based on this uncertainty, with the help of the GAMS model already introduced, it has been possible to build a sensitivity analysis on the components cost, in 13 different scenarios, showing how hydrogen storage cost influences system choices in terms of flexibility and power mix [65, 66].

The GAMS model minimize the overall system cost and it is based on several assumptions that is important to report:

- Greenfield investments are considered for every technology
- There are distribution constraints on the grid
- There is no focus on mobility and heating system, only the power grid is considered
- The considered storage options are: Li-Ion batteries, VRF batteries, H_2 above ground tanks, H_2 LRC
- Electricity production is CO_2 free: CO_2 emitting technology can exist only if CCS is applied

- Geographical distribution is only taken into account for wind generation technologies

Moreover in table 4.5 are shown the allowed technologies in the final power generation mix. Finally two different demand scenarios have been considered: a demand of raw hydrogen equal to 20% of the total electricity demand, equally distributed along all the yearly time-steps and which must be met (meaning that the hydrogen demand required is the gas amount which is possible to produce, through electrolysis, using 20% of the electricity demand), while it is also possible to produce hydrogen and burn it into fuel cells (referred in the scenarios nomenclature as "H_2 *demand*"); if not specified there is no raw hydrogen demand, as it is produced to be completely reconverted into electricity through fuel cells employment.

Technologies	Description
Gas	Combined cycle gas turbine plants
Gas peak	Open cycle gas turbines for peak power generation
WG peak	Open cycle biogas turbines for peak generation
Nuclear	Nuclear plants
Wind on shore	On shore wind turbines
PV	Photovoltaic plants
BECCS	Bio-energy CCS plants, biomass based steam boilers
FC	PEM fuel cells

Table 4.5: Model electricity production technologies

Each scenario was generated with different assumptions on the costs of hydrogen production, storage and reconversion into electricity, as well as with different demand configurations and power mix constraints: table 4.6 shows the capital cost assumption for every scenario and explains their nomenclature [75].

It is also important to notice that, since no CO_2 emissions are allowed, CO_2 emitting technologies (gas turbines) can only be employed together with BECCS plants, which in the GAMS model are supposed to compensate for CO_2 emissions from all the other producing technologies. In other words, in the "noBio" scenarios, gas turbines (open cycles or combined cycle) are not allowed, leaving hydrogen storage and fuel cells as the only flexibility measures on the grid.

For sake of simplicity, similar results in terms of technologies employment in different scenarios will be discussed within the same section in the following.

	Cheap	Original	Expensive	Super expensive
Electrolyzer[M€/MW]	0.5	1	2	-
Fuel cells[M€/MW]	0.25	0.5	1	-
LRC[k€/MWh]	-	2.5	7.5	15
Tanks[k€/MWh]	-	16.5	49.5	99
noBio	No BECCS allowed to be used for electricity generation			
Cheap H_2	Cheap electrolyzers and fuel cells			
Expensive H_2	Expensive electrolyzers and fuel cells			
Expensive storage	Both LRC and Tanks are expensive			
Both expensive	Both H_2 storages are very expensive			
Superexpensive storage	All four H_2 technologies are expensive			
H_2 demand	Hydrogen demand fixed at 20% of the electricity demand			

Table 4.6: Scenarios assumptions

4.3.1 LRC and tanks hydrogen storage

In the "Cheap H_2" and "Both expensive, H_2 demand" scenarios both hydrogen LRC and tank storages are employed, with LRC showing a seasonal behavior, while tanks show much faster charge/discharge cycles. As it can be seen in figure 4.13a, the simulation result is a relatively large dimension of LRC storage with the support of the more flexible, small capacity, tank storage option. In particular tanks can be cycled much faster than LRC storage and can thus be used to smooth the gas injection and extraction process in/from the cavern. A similar result is obtained in the scenario described in figure 4.13b: here a much smaller LRC capacity is required, justified by its high cost, while the tank capacity is comparable with the former scenario. This last scenario is useful to understand the difference between the two hydrogen storage technologies: in a scenario where hydrogen must be produced and stored to be able to cover the demand, there is the need of a large, cost effective storage option, able to cover a seasonal demand variation; however tanks provide an important flexibility measure needed by the grid operation.

4.3.2 LRC hydrogen storage

In scenarios "noBio, cheap H_2" and "Original, H_2 demand" the simulation shows that LRC is sufficient in order to respond both to flexibility and storage request. With reference to figure 4.14a, in the former scenario a very large LRC capacity is needed: based on the noBio definition discussed in the introduction to the model in section 4.3, stor-

age must be employed to respond to the flexibility needs of the grid, finding hydrogen as the best candidate among the considered storage alternatives. A direct comparison with the latter scenario, described by figure 4.14b, shows how in the latter case the LRC capacity is strongly reduced (of more than 4 times) since more flexible power generation technologies are allowed to produce electricity. However, hydrogen results to be more competitive than Li-Ion and VRF batteries, showing how hydrogen could be competitive to respond both to seasonal and a much faster electricity production variability.

4.3.3 LRC and VRF batteries storage

In several scenarios, all constrained by the "noBio" hypothesis and described in figure 4.15, the best storage mix is represented by coupling LRC with VRF batteries.

It is possible to notice a similarity in the result from the "Original, noBio" scenario and the "noBio, cheap H_2" scenario shown in figure 4.14a: the only difference here is the higher cost of hydrogen storage in the former scenario, which is reflected in the choice of a relatively small capacity of VRF, reducing the capacity of LRC. Starting from these consideration it is then possible to analyze the other scenarios, in which more expensive storage or hydrogen production and reconversion systems are considered. In particular, when considering expensive (figure 4.15d) or very expensive storage (figure 4.15b) it is possible to notice how the LRC capacity is strongly reduced in favor of a higher capacity of VRF, when the hydrogen storage cost is increased. However the system will behave in a similar way, using hydrogen to smooth seasonal variability and VRF batteries to answer to fast fluctuations on the electricity grid. It is interesting to show how, increasing electrolyzers and fuel cells costs (figure 4.15c), the LRC capacity is strongly reduced with respect to base case described by the "noBio, original" scenario: a high cost to produce and burn hydrogen will make more convenient to invest in nuclear base load, reducing the necessity for hydrogen storage capacity; on the other hand, nuclear power is not a flexible technology and there will be a strong need of flexible generation on the grid, provided by the very high capacity of VRF batteries. Finally, considering higher costs for the overall hydrogen system (electrolyzers, storage and fuel cells, figure 4.15a) will lead to a slightly lower LRC capacity (compared to the "noBio, expensive H_2" scenario, in which storage has the "original" cost): the hydrogen storage cost will also limit the employment of fuel cells, making more convenient to invest in a slightly different power production mix.

4.3.4 No hydrogen scenarios

In several scenarios the use of hydrogen technologies is not competitive, in particular:

- Both expensive
- Expensive H_2
- Expensive storage
- Original

Here only VRF batteries are employed as storage technologies, with a capacity close to 2GWh for every scenario. It easy to understand that if the the cost of the hydrogen storage or production systems is too high, when compared with alternative technologies, it is no longer convenient to invest in hydrogen. Moreover here there is not a fixed hydrogen demand to be covered, meaning that the system is not "forced" to invest in hydrogen. However the same results are obtained in the "Original" scenario, where storage costs are close to the ones found in this same study and electrolyzer and fuel cell costs are based on actual available technology. It is then possible to infer that actual hydrogen costs are not justified if there is not a hydrogen market ready to produce a raw gas demand.

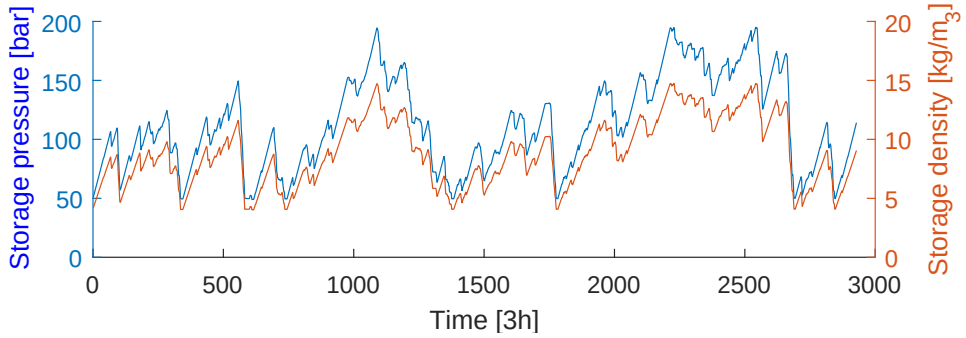

(a) p-t and ρ-t diagrams *SC*1

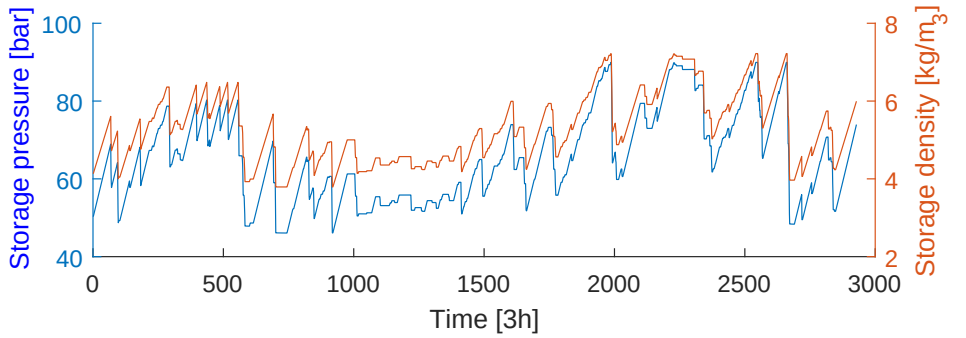

(b) p-t and ρ-t diagrams *SC*2

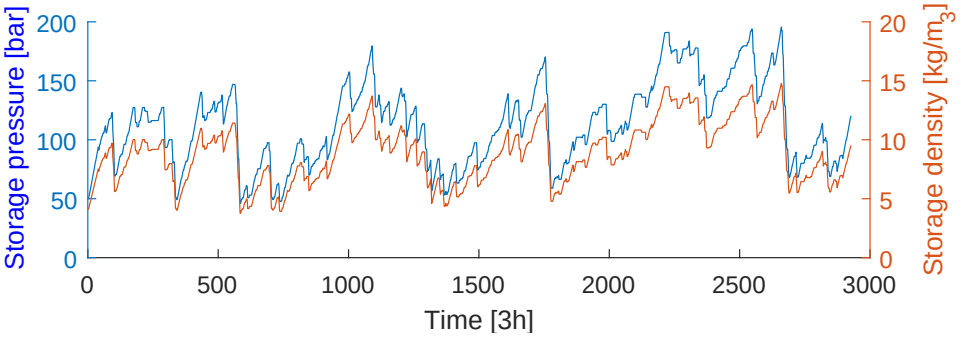

(c) p-t and ρ-t diagrams *SC*3

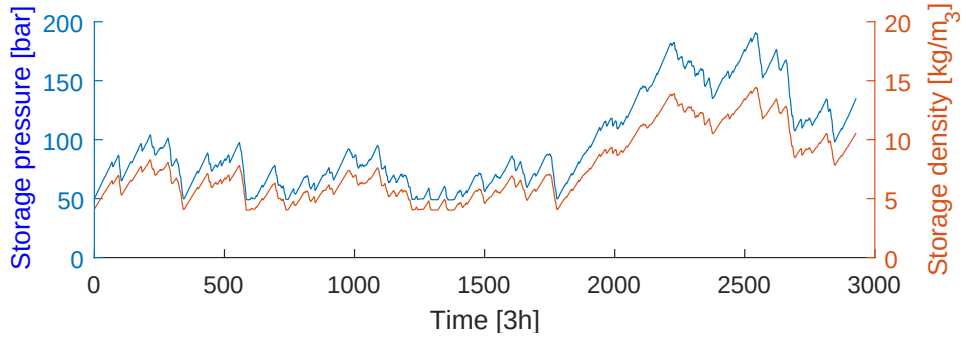

(d) p-t and ρ-t diagrams *SC*4

Figure 4.1: Pressure/Density-time diagram in the base cases

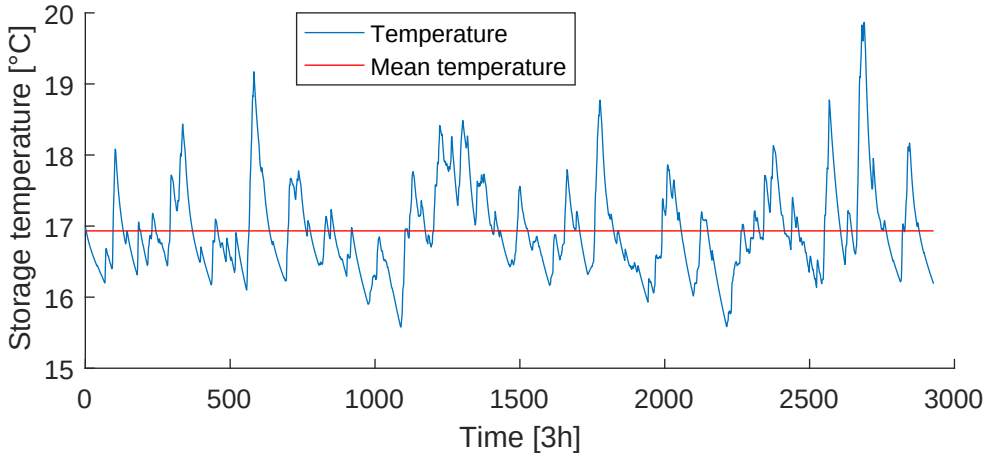

Figure 4.2: T-t diagram SC1,base

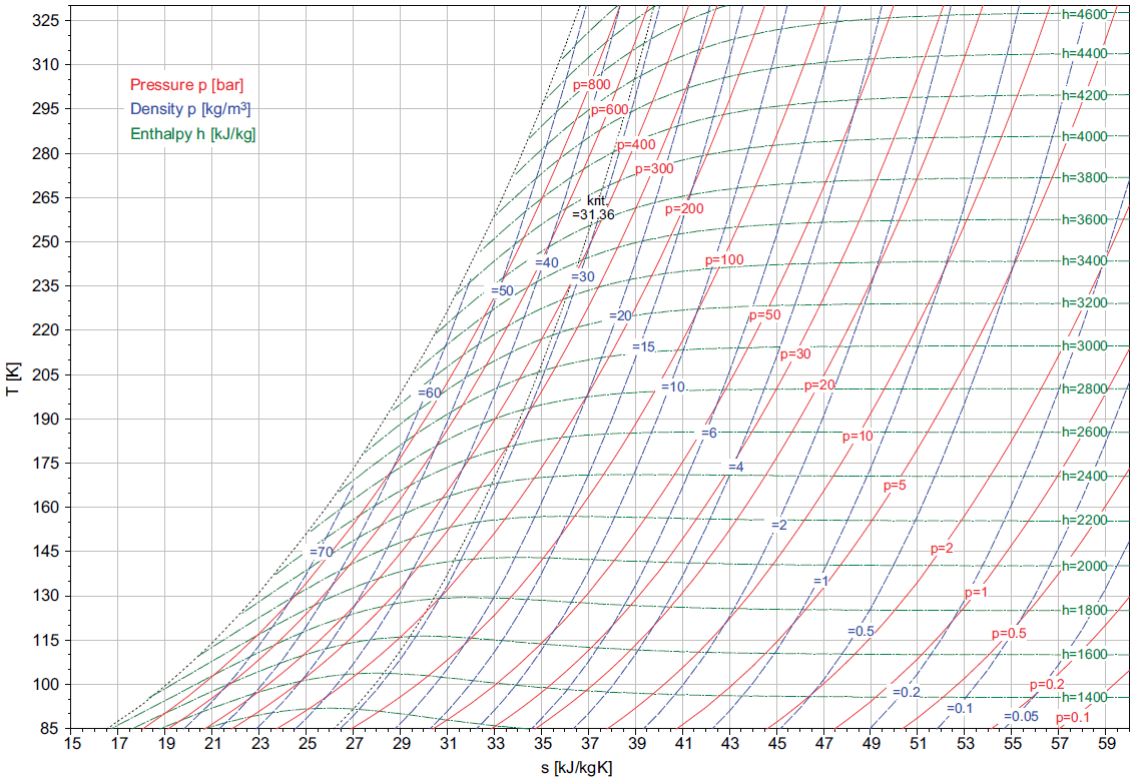

Figure 4.3: T-s diagram for equilibrium hydrogen[76]

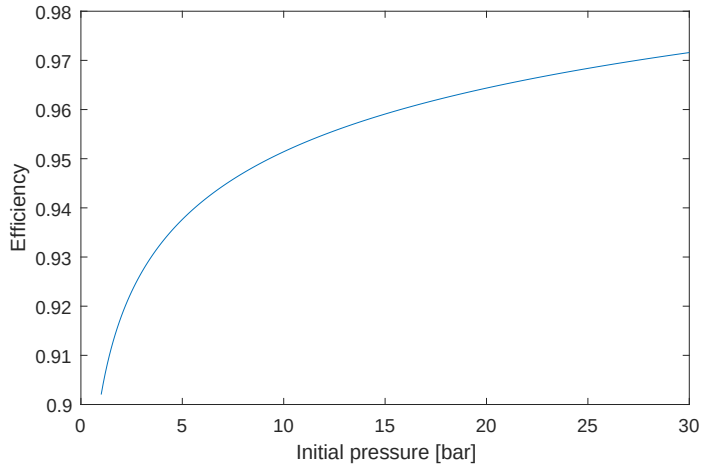

Figure 4.4: Efficiency dependence on initial compression pressure

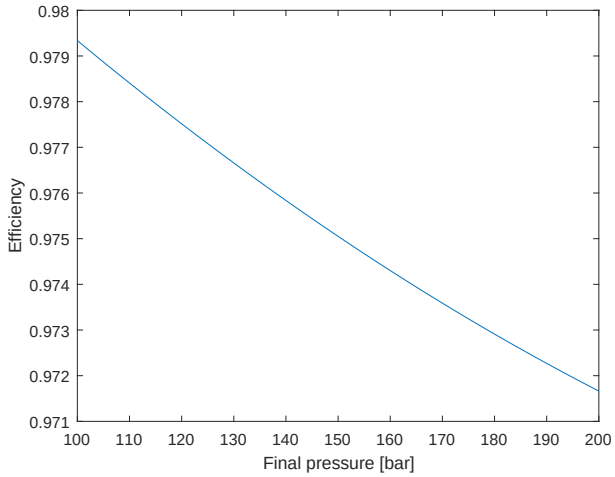

Figure 4.5: Efficiency dependence on maximum pressure

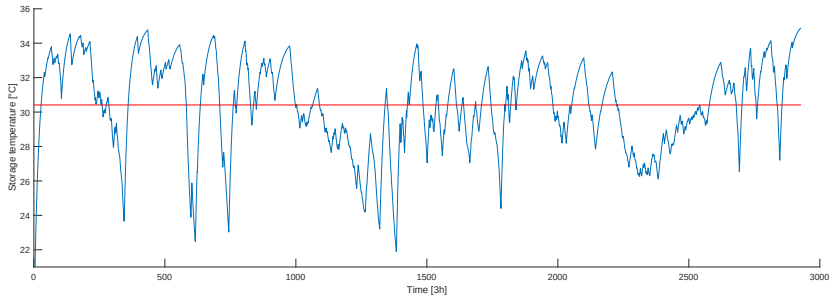

(a) T-t diagram *SC*1

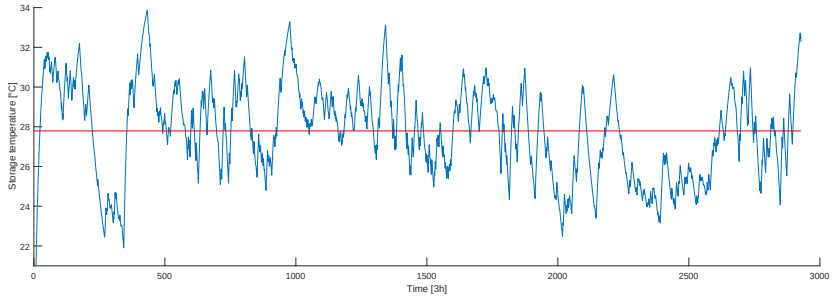

(b) T-t diagram *SC*2

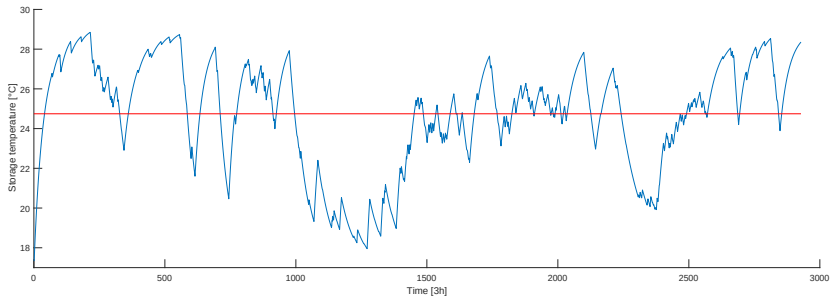

(c) T-t diagram *SC*3

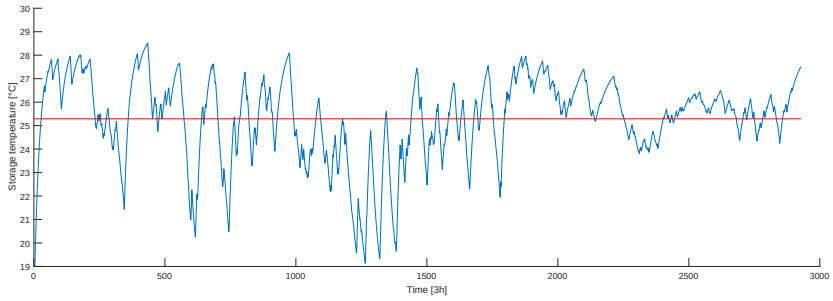

(d) T-t diagram *SC*4

Figure 4.6: T-t diagram expander cases

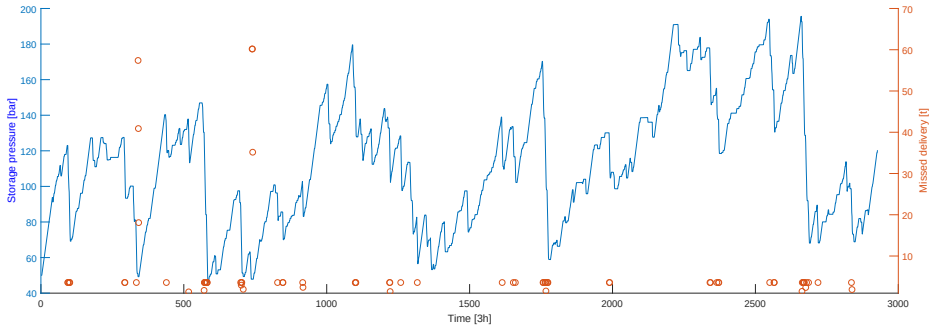

(a) Missed delivery $SC3, base$

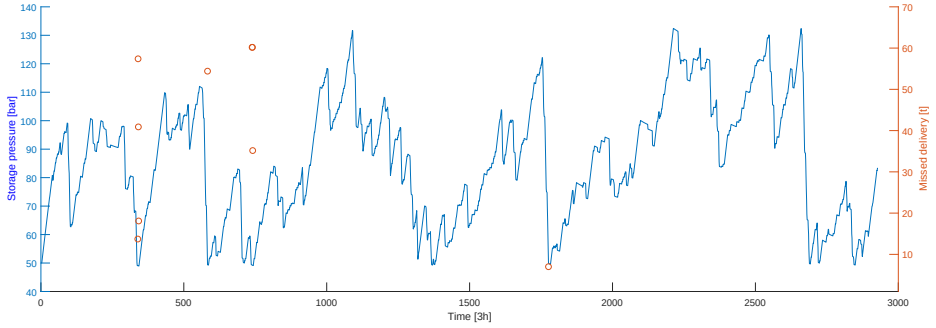

(b) Missed delivery $SC3, exp$

Figure 4.7: Missed delivery comparison

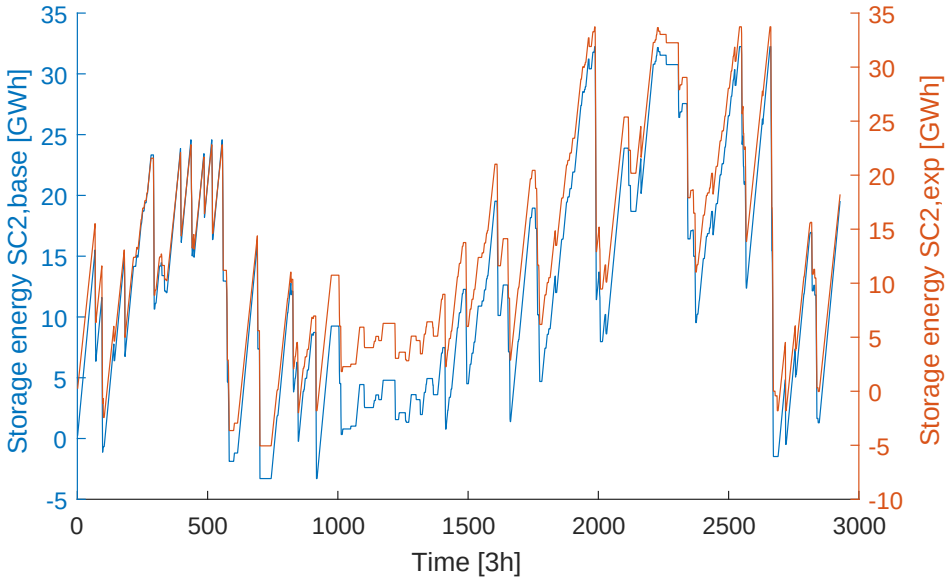

Figure 4.8: Storage energy $SC2$

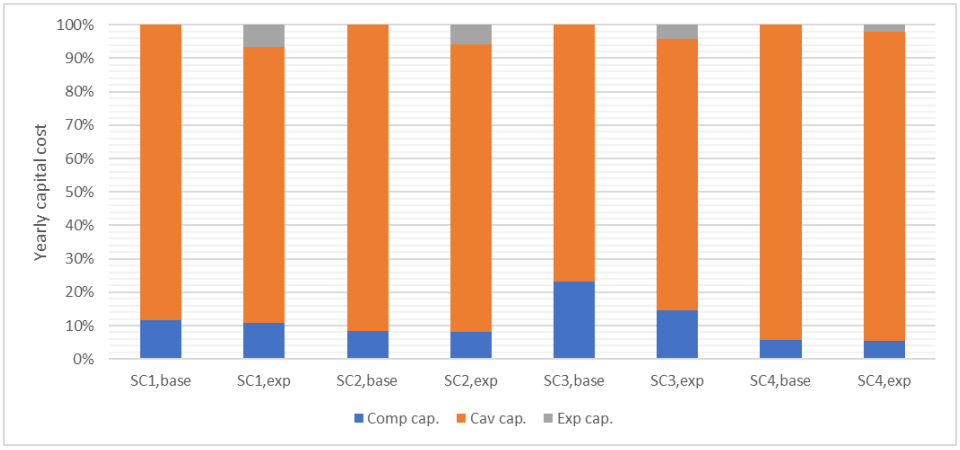

Figure 4.9: Yearly capital investment

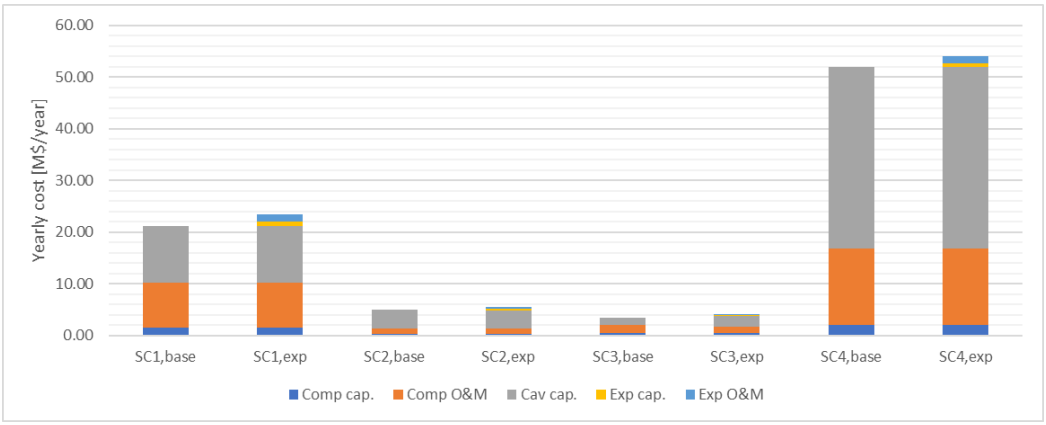

Figure 4.10: Yearly costs LRC plant

Figure 4.11: Electricity delivery costs

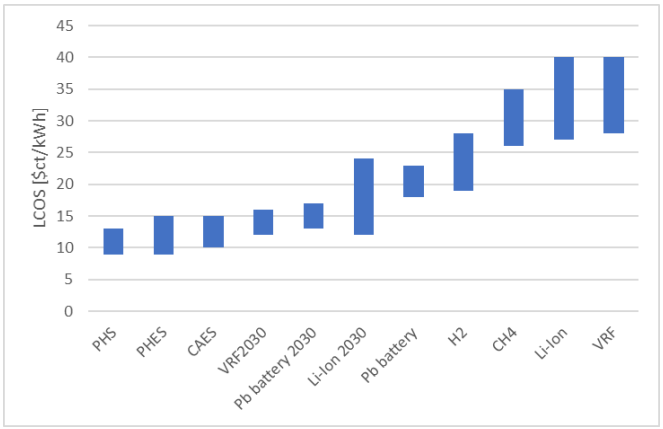

Figure 4.12: Electricity storage cost [12]

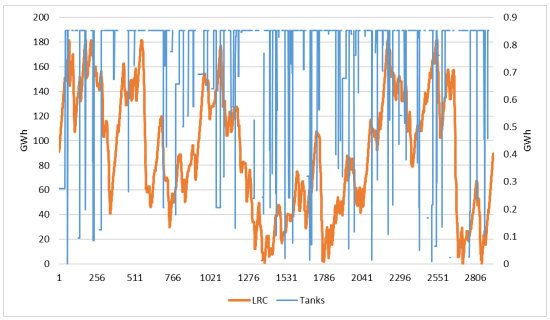

(a) Cheap H_2

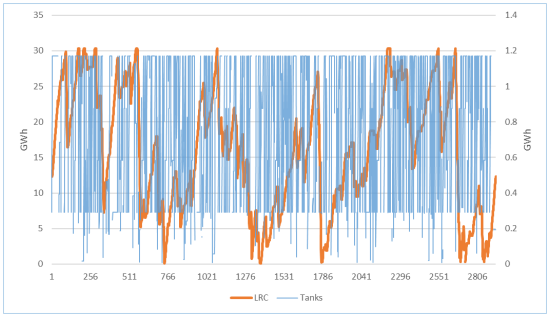

(b) Both expensive, H_2 demand

Figure 4.13: Hydrogen LRC and tanks employment scenarios

(a) noBio, cheap H_2

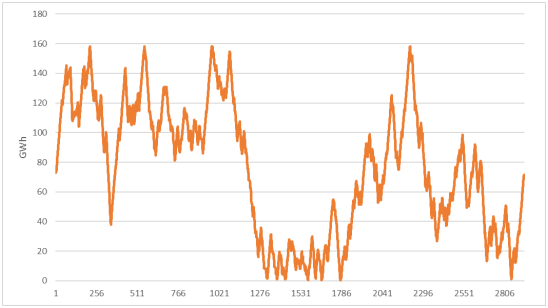

(b) Original, H_2 demand

Figure 4.14: Hydrogen LRC employment scenarios

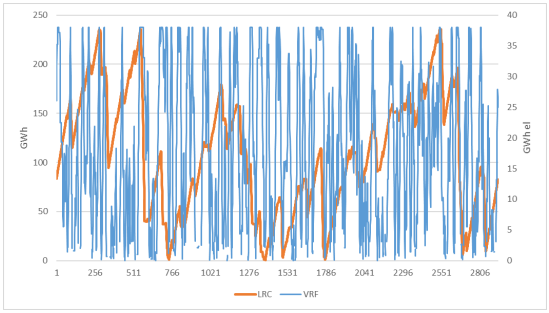

(a) noBio, both expensive

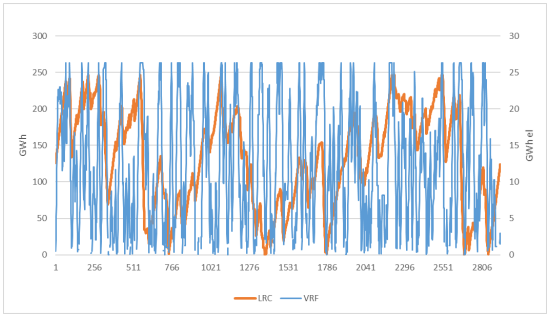

(b) noBio, superexpensive storage

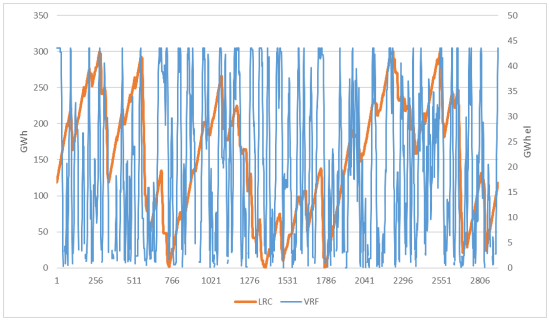

(c) noBio, expensive H_2

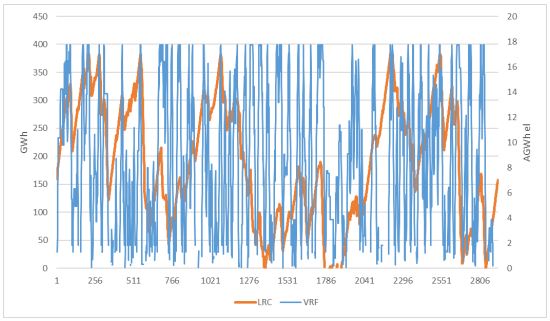

(d) noBio, expensive storage

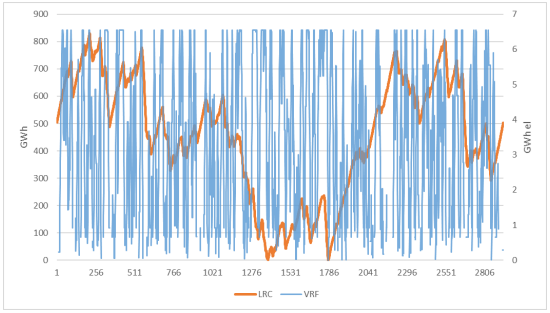

(e) noBio, original

Figure 4.15: LRC and VRF batteries employment scenarios

Chapter 5

Conclusions

In a near future with a growing share of renewables and increased attention to CO_2 emission reduction, energy storage seems to be one of the most reliable flexibility measure for power grid support. The unique assessed large scale storage solution is PHS, which is not still able to provide seasonal storage; CAES systems are now under development and they could provide a valid storage alternative in geological suitable regions. On the other hand compressed hydrogen storage, in the form of underground Lined Rock Cavern, could provide higher storage capacity thanks to its intrinsic gas nature. This technology could help the integration of wind and PV plants into the grid thanks to the employment of water electrolyzers to produce hydrogen during low demand periods. Once stored, hydrogen could be then delivered as raw material for industry and mobility or reconverted into electricity, through the use fuel cells or gas turbines, to feed the grid during peak demand.

LRC systems are not a mature technology, but they mainly rely on well known practices, as the cavern excavation process and hydrogen compression and handling from chemical industry applications. Moreover one lined cavern for natural gas storage is already in operation in Skallen, Sweden, and more are being tested in Japan and Korea. Thanks to the dimension of the caverns, their excavation modularity and the high energy density of hydrogen (when compared with air), LRC can provide storage capacities of hundreds of GWh with a low environmental impact. The development of PEM electrolyzers, able to perform well during variable operation, will lead to a cost reduction of the technology which in turn could lead to make hydrogen produced from electrolysis competitive with traditional production technologies. Finally the development of a sustainable hydrogen market would help with its delivery as raw material, avoiding its expensive reconversion into electricity. In this direction, mobility would be the hydrogen economy driver, leaving P2G with a marginal role.

In this study an ideal storage system have been considered: hydrogen produced from a PEM electrolyzer is fed to a cluster of LRC and, when needed, it is expanded to match the distribution pipeline pressure. A model studing the injection, static storage, withdrawal process and the eventual expansion in a turboexpander has been developed in Matlab. The input data for the model, in the form of hydrogen production and demand in different scenarios, were taken from a power grid cost optimization model developed by Chalmers University of Technology. The model developed in this study was able to simulate one year of storage operation, giving as results gas properties trends and system costs. These costs have been later compared with other storage technologies to understand the competitiveness of hydrogen LRC systems.

The thermodynamic analysis led to the description of the storage operation in terms of evolution of the physical characteristics of the gas inside the caverns, the efficiency of the charge-discharge cycle and the possible energy recovery from a turboexpander at the cavern outlet. LRCs show a seasonal utilization of the storage since there are limits on the maximum gas injection and withdrawal; high system efficiency in the order of $97-98\%$; low recovery efficiency of the turboexpander, which makes its installation not cost effective in the considered scenarios. The cost analysis was performed on a lifetime of 25 years and led to the definition of a system and delivery cost for hydrogen. The storage system capital cost was dominated by the cavern excavation cost, while the yearly cost was also strongly influenced by the electricity cost to drive the compressor. Those costs have been compared with other compressed hydrogen storage technologies, resulting in a lower delivery cost when considering cavern cyclability. Moreover hydrogen resulted to be competitive with battery storage applications, even when considering the full cost of electricity for hydrogen production; when hydrogen is produced from cheap off peak electricity, the cost of electricity delivery could be as low as $0.11-0.12\,\$/\mathrm{kWh_{el}}$ in the ideal case of free electricity availability, being competitive with PHS and CAES in the actual conditions and going below those values, when 2025 costs for the electrolysis process are considered. Finally the impact of LRC cost on the electricity system has been studied, thanks to a sensitivity analysis on the hydrogen technologies in different future scenarios, with the help of the GAMS model developed by Chalmers University of Technology. Scenarios analysis has shown that LRC storage would be employed only if poor flexible generation is allowed on the grid and/or in the case of a fixed raw hydrogen demand.

Hydrogen storage LRC systems have the potential to provide large-scale seasonal storage to support the integration of renewables on the power grid. The high storage capacity, the possibility of reconverting hydrogen into electricity through the use of fuel cells or traditional gas turbines, the potential future market for raw hydrogen for mobility or P2G applications are the drivers of this technology. However strong efforts must be made to reduce costs related to electrolysis and electricity production: in particular hydrogen produced from electrolysis is still not competitive with traditional production technologies. In a future with very stringent constraints on the power mix, hydrogen could be a suitable storage solution.

List of Figures

List of Tables

Nomenclature

AA-CAES Advanced Adiabatic Compressed Air Energy Storage

AEL Alkaline electrolyzer

ATR Autothermal Reforming

BECCS Bio-energy Carbon Capture and Storage

BEV Battery Electric Vehicles

CAES Compressed Air Energy Storage

CCS Carbon Capture and Storage

CG Coal Gasification

FCV Fuel Cell Vehicles

GHG GreenHouse Gases

H2ICE Hydrogen Interna Combustion Engine

LHV Lower Heating Value

Li-ion Lithium-ion

LRC Lined Rock Cavern

NPC Net Present Cost

P2G Power To Gas

PEM Polymer Electrolyte Membrane

PHS Pumped Hydroelectric Storage

PV Photovoltaic

RES Renewable Energy Sources

SMES Superconductive Magnetic Energy Storage

SMR Steam Methane Reforming

SOEL Solid oxide electrolyzer

VRF Vanadium Redox Flow

Bibliography

[1] Herib Blanco and André Faaij. A review at the role of storage in energy systems with a focus on Power to Gas and long-term storage. *Renewable and Sustainable Energy Reviews*, 81(July 2017):1049–1086, 2018.

[2] IEA. *World Energy Outlook 2015*. OECD Publishing, 2015.

[3] Holli Riebeek. Global Warming, 2010.

[4] British Petroleum. BP Statistical Review of World Energy 2017. *British Petroleum*, (66):1–52, 2017.

[5] U. Bünger, J. Michalski, F. Crotogino, and O. Kruck. *Large-scale underground storage of hydrogen for the grid integration of renewable energy and other applications*. Elsevier Ltd., 2016.

[6] A. A. Solomon, Daniel M. Kammen, and D. Callaway. The role of large-scale energy storage design and dispatch in the power grid: A study of very high grid penetration of variable renewable resources. *Applied Energy*, 134:75–89, 2014.

[7] Xing Luo, Jihong Wang, Mark Dooner, and Jonathan Clarke. Overview of current development in electrical energy storage technologies and the application potential in power system operation. *Applied Energy*, 137:511–536, 2015.

[8] J. P. Deane, B. P. Ó Gallachóir, and E. J. McKeogh. Techno-economic review of existing and new pumped hydro energy storage plant. *Renewable and Sustainable Energy Reviews*, 14(4):1293–1302, 2010.

[9] Larissa De Souza Noel Simas Barbosa, Javier Farfan Orozco, Dmitrii Bogdanov, Pasi Vainikka, and Christian Breyer. Hydropower and Power-to-gas Storage Options: The Brazilian Energy System Case. *Energy Procedia*, 99(March):89–107, 2016.

[10] Daniel Fraile, Jean-Christophe Lanoix, Patrick Maio, Azalea Rangel, and Angelica Torres. Overview of the market segmentation for hydrogen across potential customer groups based on key application areas. (1):1–32, 2015.

[11] R. Debarre, B. Decourt, and B. Lajoie. Hydrogen based energy-conversion FactBook. *SBC Energy Institute*, (February), 2014.

[12] D Steward, G Saur, M Penev, and T Ramsden. Lifecycle Cost Analysis of Hydrogen Versus Other Technologies for Electrical Energy Storage Lifecycle Cost Analysis of Hydrogen Versus Other Technologies for Electrical Energy Storage. *Contract*, (November), 2009.

[13] Mandhapati Raju and Siddhartha Kumar Khaitan. System simulation of compressed hydrogen storage based residential wind hybrid power systems. *Journal of Power Sources*, 210:303–320, 2012.

[14] Guido Plebmann, Matthias Erdmann, Markus Hlusiak, and Christian Breyer. Global energy storage demand for a 100% renewable electricity supply. *Energy Procedia*, 46:22–31, 2014.

[15] E. Kotter, L. Schneider, F. Sehnke, K. Ohnmeiss, and R. Schroer. Sensitivities of power-to-gas within an optimised energy system. *Energy Procedia*, 73:190–199, 2015.

[16] Andreas Palzer and Hans Martin Henning. A comprehensive model for the German electricity and heat sector in a future energy system with a dominant contribution from renewable energy technologies - Part II: Results. *Renewable and Sustainable Energy Reviews*, 30:1019–1034, 2014.

[17] Stephen Clegg and Pierluigi Mancarella. Integrated modelling and assessment of the operational impact of power - to - gas (P2G) on electrical and gas transmission networks. *IEEE Trans Sust Energy. 6, (4)*, 6(4):1234–44, 2015.

[18] Dmitrii Bogdanov and Christian Breyer. North-East Asian Super Grid for 100% renewable energy supply: Optimal mix of energy technologies for electricity, gas and heat supply options. *Energy Conversion and Management*, 112:176–190, 2016.

[19] Paolo Chiesa, Giovanni Lozza, and Luigi Mazzocchi. Using Hydrogen as Gas Turbine Fuel. *Journal of Engineering for Gas Turbines and Power*, 127(1):73, 2005.

[20] Joshua Eichman, Aaron Townsend, and Marc Melaine. Economic Assessment of Hydrogen Technologies Participating in California Electricity Markets. *National Renewable Energy Laboratory*, (February):31, 2016.

[21] A. I. Schastlivtsev and O. V. Nazarova. Hydrogen air energy storage gas-turbine system. *Thermal Engineering*, 63(2):107–113, 2016.

[22] Ibrahim Dincer and Canan Acar. Review and evaluation of hydrogen production methods for better sustainability. *International Journal of Hydrogen Energy*, 40(34):11094–11111, 2014.

[23] C. Acar and I. Dincer. Comparative environmental impact evaluation of hydrogen production methods from renewable and nonrenewable sources. *Causes, impacts and solutions to global warming*, 39(1):493–514, 2013.

[24] Susan Schoenung. Economic Analysis of Large-Scale Hydrogen Storage for Renewable Utility Applications. *Sandia Report*, (August):1196–1199, 2011.

[25] Alexander Buttler and Hartmut Spliethoff. Current status of water electrolysis for energy storage, grid balancing and sector coupling via power-to-gas and power-to-liquids: A review. *Renewable and Sustainable Energy Reviews*, (February), 2017.

[26] EIA, 2017.

[27] Andrew Smallbone, Verena Jülch, Robin Wardle, and Anthony Paul Roskilly. Levelised Cost of Storage for Pumped Heat Energy Storage in comparison with other energy storage technologies. *Energy Conversion and Management*, 152(May):221–228, 2017.

[28] Verena Jülch. Comparison of electricity storage options using levelized cost of storage (LCOS) method. *Applied Energy*, 183:1594–1606, 2016.

[29] Anna S Lord, Peter H Kobos, Geoffrey T Klise, and David J Borns. A Life Cycle Cost Analysis Framework for Geological Storage of Hydrogen: A User's Tool. *Analysis*, (September):1–60, 2011.

[30] Fan Zhang, Pengcheng Zhao, Meng Niu, and Jon Maddy. The survey of key technologies in hydrogen energy storage. *International Journal of Hydrogen Energy*, 41(33):14535–14552, 2016.

[31] Claus Jorgensen and Stephanie Ropenus. Production price of hydrogen from grid connected electrolysis in a power market with high wind penetration. *International Journal of Hydrogen Energy*, 33(20):5335–5344, 2008.

[32] Battelle Memorial Institute. Manufacturing Cost Analysis of 100 and 250 kW Fuel Cell Systems for Primary Power and Combined Heat and Power Applications. *DOE Report*, (January), 2016.

[33] Hyung Mok Kim, Jonny Rutqvist, Dong Woo Ryu, Byung Hee Choi, Choon Sunwoo, and Won Kyong Song. Exploring the concept of compressed air energy storage (CAES) in lined rock caverns at shallow depth: A modeling study of air tightness and energy balance. *Applied Energy*, 92:653–667, 2012.

[34] Y. Huang, P. Keatley, H.S. Chen, X.J. Zhang, A. Rolfe, and N.J. Hewitt. Techno-economic study of compressed air energy storage systems for the grid integration of wind power. *International Journal of Energy Research*, (July 2017):559–569, 2017.

[35] Chi Jen Yang. Pumped Hydroelectric Storage. *Storing Energy: With Special Reference to Renewable Energy Sources*, pages 25–38, 2016.

[36] DOE. DOE Global Energy Storage Database, 2017.

[37] S.M. Schoenung and W.V. Hassenzahl. Long- vs . Short-Term Energy Storage Technologies Analysis A Life-Cycle Cost Study A Study for the DOE Energy Storage Systems Program. *Sandia Report*, SAND2011-2(August):84, 2003.

[38] F. Geth, T. Brijs, J. Kathan, J. Driesen, and R. Belmans. An overview of large-scale stationary electricity storage plants in Europe: Current status and new developments. *Renewable and Sustainable Energy Reviews*, 52:1212–1227, 2015.

[39] Chao Zhang, Yi Li Wei, Peng Fei Cao, and Meng Chang Lin. Energy storage system: Current studies on batteries and power condition system. *Renewable and Sustainable Energy Reviews*, 82(October 2017):3091–3106, 2018.

[40] Ahmet Ozarslan. Large-scale hydrogen energy storage in salt caverns. *International Journal of Hydrogen Energy*, 37(19):14265–14277, 2012.

[41] Sofregaz US Inc. and LRC. Commercial Potential of Natural Gas Storage in Lined Rock Caverns (Lrc). Technical report, U.S. Department fo Energy Federal Energy Technology Center, 1999.

[42] Yingjie Yan, Yu Yan, Yang He, Jinxu Li, Yanjing Su, and Lijie Qiao. Hydrogen-induced cracking and service safety evaluation for precipitation strengthened austenitic stainless steel as hydrogen storage tank. *International Journal of Hydrogen Energy*, 39(31):17921–17928, 2014.

[43] Dohyun Park, Hyung Mok Kim, Dong Woo Ryu, Byung Hee Choi, and Kong Chang Han. Probability-based structural design of lined rock caverns to resist high internal gas pressure. *Engineering Geology*, 153:144–151, 2013.

[44] Bojan Žlender and Stojan Kravanja. Cost optimization of the underground gas storage. *Engineering Structures*, 33(9):2554–2562, 2011.

[45] Rune Glamheden and P. Curtis. Excavation of a cavern for high-pressure storage of natural gas. *Tunnelling and Underground Space Technology*, 21(1):56–67, 2006.

[46] Alfredo Ursúa, Luis M. Gandía, and Pablo Sanchis. Hydrogen production from water electrolysis: Current status and future trends. *Proceedings of the IEEE*, 100(2):410–426, 2012.

[47] A. S. Aricò, S. Siracusano, N. Briguglio, V. Baglio, A. Di Blasi, and V. Antonucci. Polymer electrolyte membrane water electrolysis: Status of technologies and potential applications in combination with renewable power sources. *Journal of Applied Electrochemistry*, 43(2):107–118, 2013.

[48] Frano Barbir. PEM electrolysis for production of hydrogen from renewable energy sources. *Solar Energy*, 78(5):661–669, 2005.

[49] Mustafa Serdar Genç, Muhammet Çelik, and Ilyas Karasu. A review on wind energy and wind-hydrogen production in Turkey: A case study of hydrogen production via electrolysis system supplied by wind energy conversion system in Central Anatolian Turkey. *Renewable and Sustainable Energy Reviews*, 16(9):6631–6646, 2012.

[50] Raúl Sarrias-Mena, Luis M. Fernández-Ramírez, Carlos Andrés García-Vázquez, and Francisco Jurado. Electrolyzer models for hydrogen production from wind energy systems. *International Journal of Hydrogen Energy*, 40(7):2927–2938, 2015.

[51] Christoph Rakousky, Uwe Reimer, Klaus Wippermann, Susanne Kuhri, Marcelo Carmo, Wiebke Lueke, and Detlef Stolten. Polymer electrolyte membrane water electrolysis: Restraining degradation in the presence of fluctuating power. *Journal of Power Sources*, 342:38–47, 2017.

[52] Martin Linder. The role of Battery Electric Vehicles, Plug-in Hybrids and Fuel Cell Electric Vehicles. *Fuel Cell*, page 68, 2010.

[53] Iea. Technology Roadmap. *SpringerReference*, page 81, 2015.

[54] Sandro Pellegrino, Andrea Lanzini, and Pierluigi Leone. Greening the gas network - The need for modelling the distributed injection of alternative fuels. *Renewable and Sustainable Energy Reviews*, 70(November 2016):266–286, 2017.

[55] API. Reciprocating Compressors for Petroleum, Chemical, and Gas Industry Services, API Standard 618. page 4th Ed. June, 1995.

[56] DOE. H2A Delivery Components Model Version 1 . 1 : Users Guide. *U.S Department Of Energy*, 2006.

[57] J. W. Leachman, R. T. Jacobsen, S. G. Penoncello, and E. W. Lemmon. Fundamental equations of state for parahydrogen, normal hydrogen, and orthohydrogen. *Journal of Physical and Chemical Reference Data*, 38(3):721–748, 2009.

[58] M Conte. Hydrogen Economy. *ABB Switzerland Ltd*, pages 232–254, 2009.

[59] Carriveau and Ting, editors. *Methane and Hydrogen for Energy Storage*. Number February. Institution of Engineering and Technology, jul 2016.

[60] S. A. Sherif, F. Barbir, and T. N. Veziroglu. Wind energy and the hydrogen economy-review of the technology. *Solar Energy*, 78(5):647–660, 2005.

[61] Bojan Žlender, Primož Jelušič, and Djamalddine Boumezerane. The feasibility analysis of underground gas storage caverns. *Engineering Structures*, 55:16–25, 2013.

[62] Olaf Kruck. Assessment of the potential, the actors and relevant business cases for large scale and seasonal storage of renewable electricity by hydrogen underground storage in Europe. (June), 2014.

[63] J. Johansson. High Pressure Storage of Gas in Lined Rock Caverns, Cavern Wall Design Principles. 2003.

[64] Jun Nobuto, Yoshio Ishizuka, Kazuo Sawa, Etuo Niwa, Hisashi Kagawa, and Yoshito Umeda. Study on lined rock gas storage technology in Japan. (22):14, 2000.

[65] Lisa Göransson, Joel Goop, Mikael Odenberger, and Filip Johnsson. Impact of thermal plant cycling on the cost-optimal composition of a regional electricity generation system. *Applied Energy*, 197:230–240, 2017.

[66] Viktor Johansson and Lisa Göransson. Impacts of variation management on cost-optimal investments in wind power and solar photovoltaics. *Submitted for journal publication*.

[67] C. D. Pérez-Segarra, J. Rigola, M. Sòria, and A. Oliva. Detailed thermodynamic characterization of hermetic reciprocating compressors. *International Journal of Refrigeration*, 28(4):579–593, 2005.

[68] Dennis Roskosch, Valerius Venzik, and Burak Atakan. Thermodynamic model for reciprocating compressors with the focus on fluid dependent efficiencies. *International Journal of Refrigeration*, 84:104–116, 2017.

[69] Ramesh K Shah and Dusan P. Seculic. *Fundamentals of heat exchanger design*. 2003.

[70] Andrzej Witkowski, Andrzej Rusin, Mirosław Majkut, and Katarzyna Stolecka. Comprehensive analysis of hydrogen compression and pipeline transportation from thermodynamics and safety aspects. *Energy*, pages 1–11, 2016.

[71] R R Aghai, M C Lin, and B Ershaghi. Improvements of the efficiency of the turboexpanders in cryogenic applications. 41:933–940, 1996.

[72] Ebrahim Khalili Ardali, Esmaeil Heybatian, Bakhtiari Province, and Gas Company. Stations By Use of Gas Turbo Expander ; Evaluation of Available. pages 1–6, 2008.

[73] Originator Chris Ainscough, David Peterson, and Eric Miller. Hydrogen production cost from PEM electrolysis. *Ainscough,Chris Petersonm, David Miller, Eric Satyapal, Sunita*, pages 1–11, 2014.

[74] Thamir k. Ibrahim, Mohammed Kamil, Omar I. Awad, M. M. Rahman, G. Najafi, Firdaus Basrawi, Ahmed N. Abd Alla, and Rizalman Mamat. The optimum performance of the combined cycle power plant: A comprehensive review. *Renewable and Sustainable Energy Reviews*, 79(May):459–474, 2017.

[75] Energinet.dk. *TECHNOLOGY DATA FOR ENERGY PLANTS - Generation of Electricity and District Heating, Energy Storage and Energy Carrier Generation and Conversion*. 2012.

[76] Manfred Klell. *Storage of Hydrogen in the Pure Form*. 2010.

[77] Srikkanth Ramachandran and Ulrich Stimming. Well to wheel analysis of low carbon alternatives for road traffic. *Energy Environ. Sci.*, 8(11):3313–3324, 2015.

[78] Matthew a Kromer and John B Heywood. Electric Powertrains: Opportunities and Challenges in the U.S. Light-Duty Vehicle Fleet. *Challenges*, (May):153, 2007.

[79] John German. Electric Vehicles : Performance , Cost , Penetration. *CCAP MAIN-Latin American Regional Dialogue*, 2014.